Scientific Committee
Sixteenth Regular Session

11-20 August 2020

Assessing trends in skipjack tuna abundance from purse seine catch and effort data in the WCPO

WCPFC-SC16-2020/SA-IP-09 Rev 1

Tiffany Vidal[1], Paul Hamer[1], Lauriane Escalle[1], Graham Pilling[1]

Revision 1: Corrections made to equation for Area Occupied statistics, as well as to associated text. In addition, subscripts were added to the equation describing the minimum area to produce 90% of the catch (D90), for clarification.

[1]Oceanic Fisheries Programme (OFP), The Pacific Community, Nouméa, New Caledonia

Contents

Executive Summary

Developing a reliable index of relative abundance for skipjack, to inform the assessment model on trends through time, is a priority given the contraction of the pole-and-line fishery. Catch rates from the pole-and-line fishery have been a key input into the skipjack assessment models in the past, but the fishery's ability to provide the spatial and temporal coverage needed to adequately assess changes in abundance has clearly degraded over time. The purse seine fleet is now the major contributor to skipjack removals in the WCPO, and therefore, may serve as the best source of information with which to continue monitoring and assessing skipjack trends. This paper describes a spatiotemporal modeling approach for skipjack catch rate data collected by fishery observers for the purse seine fishery. The main objective is to determine the potential of this approach to provide a suitable relative abundance index for skipjack in the tropical WCPO.

Within the modeling framework, we have evaluated a suite of catchability covariates related to vessel, gear, and fishing strategy characteristics. These covariates were 'standardized out' of the model, to remove their effect on catch rates, and produce an index that is assumed to be representative of the trends in skipjack abundance. In addition, the modeling framework we have used allows for the inclusion of habitat covariates, predicted to influence relative skipjack density; the model estimates are therefore conditioned upon these covariates. The model presented here included vessel length, set type (i.e. associated with fish aggregating devices (FADs) or unassociated free-schools), and a species composition cluster variable as catchability covariates, and the El Niño Southern Oscillation index as a proxy covariate for spatiotemporal variation in preferred oceanic habitat conditions. The estimated regional abundance indices suggested that skipjack biomass has been relatively stable over the time series evaluated, 2010-2018.

Given concerns about potential hyperstability of a purse seine based CPUE abundance index, we developed a suite of indicators, separate from the CPUE data, to provide a more holistic representation of skipjack trends through time. This information was intended to lend support to the inference from the CPUE analysis, if agreement was detected, or to highlight concerns with the CPUE indices, if the information was in disagreement. We have presented a suite of spatial distribution metrics (SDMs), developed from self-reported logsheet data, from 2000-2018. We evaluated metrics associated with occupancy, aggregation, quantity, and distribution; and assessed these metrics against biomass estimated from the previous stock assessment, with respect to ecological theory. The SDMs were calculated separately for FAD and free-school sets, in an attempt to highlight differences based on fishing strategy. Area occupied (fishing locations where skipjack were caught) increased for both set types over the time series, as did the minimum area required to account for 90% of the catch. Ecological theory would suggest that an increase in these metrics is inconsistent with a significant decrease in biomass because they suggest spatial dispersion as opposed to contraction into areas of optimal habitat, as would be expected for a depleted population. The Gini index associated with aggregation, which provides a measure of the spatial patchiness of catches, remained fairly stable over the time series, suggesting that patchiness of tuna schools has not changed substantially. Lastly, we evaluated the proportion of sets with catches classified as 'high', relative to catches for the time series. The proportion of high skipjack catches was predicted to be positively correlated with abundance. The FAD sets showed an increase

in proportion of high catch sets, whereas the free-school sets showed a modest decline.

In addition to the SDMs, we were interested in assessing trends in the center of gravity and inertia of the skipjack distribution. Using logsheet data from 2000-2018, the center of gravity demonstrated a slight shift south and east through time, an observation which may be related to the prevalence of El Niño conditions over much of the past two decades. Aside from inter-annual shifts in the center of the distribution, as well as the inertia around the distribution, there were no obvious patterns in the location or expansion/contraction of the distribution. These conclusions are largely qualitative at this point, and presented to serve as context for the CPUE-based trends. The length frequency data showed inter-annual variability in the mode, but lacked directional shifts in the distribution and did not suggest truncation of the size-structure over the time series.

The data and modeling results presented here suggest that over the recent time series, 2010-2018, the skipjack population has been relatively stable. Ensuring reliability of the indices and metrics presented are important for the continued sustainable management of skipjack tuna in the WCPO. The CPUE standardization model described here is provided as a base case model to inform the next skipjack assessment on abundance trends, but also as a platform from which to evaluate additional analyses related to effort creep, FAD activity, and climate change. Incorporation of purse seine catch rate data into the assessment and monitoring of skipjack is paramount, and continued development of approaches to do so remains a high priority.

We invite WCPFC-SC16 to note the results of this analysis and recommendations for future research:

Results

- This analysis presents a spatiotemporal model to standardize purse seine CPUE to better inform the stock assessment models on skipjack abundance trends, across the main spatial domain of the purse seine fishery.
- A suite of spatial distribution metrics have been explored as abundance indicators to buffer against uncertainty associated with a potentially hyperstable CPUE index.
- Over the time series evaluated (2010-2018) skipjack tuna abundance trends appear to be relatively stable, and the SDMs lend support to this result.
- Vessel, gear, and fishing strategy characteristics have been included in the model to capture variability associated with effort creep in the fishery; however, additional research is recommended to better address these changes.

Recommendations

- Prioritize continued research on the development of reliable indicators and proxies from purse seine catch and effort data to monitor trends in skipjack tuna abundance.

- Support continued research focused on developing methods to more reliably measure effort creep, including a fisher survey to better understand factors that have contributed to efficiency changes in the purse seine fishery over time; information which will help refine hypotheses and analytical methods to quantify effort creep.
- Explicitly evaluate the impacts of FADs on changes in catch rates and distribution of tropical tunas. Specifically, evaluate the influence of FAD density on catch rates, and explore the ecological-trap hypothesis with respect to the distribution of tropical tunas and drifting FADs. In addition, explore the use of FAD-echo sounder data as a source of presence/absence data to be used in conjunction with CPUE data, to better inform the model on 'known' absences in unfished strata.
- Explore the utility of VMS data to redefine the effort metric in the purse seine fishery. These data could be used to understand changes in fishing behaviors and searching patterns over time, changes potentially related to technological creep and efficiency gains.
- Recognize the importance of continued research on tuna biology and demographic processes such as age/length compositions and maturation, and changes in these processes over time for improved monitoring of skipjack.

1 Introduction

Globally, it is estimated that bottom trawling and purse seining jointly account for more than half of marine fisheries catches in recent years, with the purse seine sector contributing to approximately 29% of global harvest (Cashion et al., 2018). The western and central Pacific Ocean (WCPO) supports the world's largest and most valuable tuna fishery in the world. In 2018, harvest from the Western and Central Pacific Fisheries Commission Convention Area (WCPFC-CA) comprised 55% of the global tuna harvest (4.9 mill mt), of which 71% was harvested by the purse seine fleet (Williams and Reid, 2019). Despite the substantial and growing contribution of purse seine harvest to global tuna removals, purse seine catch and effort time series have rarely been incorporated into tuna stock assessment models (but see Bigelow et al., 2019; Vidal et al., 2019). This absence is largely due to the perceived hyperstability in purse seine catch rates.

Quantitative stock assessment models often serve as the basis for sustainable management by providing an assessment of population abundance and trends. Relative abundance indices serve as a key input into stock assessment models, and are typically derived from design-based research surveys or from catch and effort data from commercial fisheries, when fishery-independent surveys are unavailable or impractical. Due to the fact that fishery data are not random, as fishers intentionally target areas of high fish density, these data must be standardized prior to use in assessment models to remove factors influencing catch rates, other than underlying abundance trends (Hilborn and Walters, 1992). Effectively standardizing purse seine catch per unit effort (CPUE) data is particularly challenging because fishing effort is concentrated on schooling aggregations of fish, and therefore the potential for catch rates to remain high while abundance declines (i.e. hyperstability) is an important concern.

Hyperstability has been implicated in masking population declines, and in some cases, the collapse of fisheries (Rose and Kulka, 1999; Erisman et al., 2011; Hamilton et al., 2016), and is largely associated with fisheries that target predictable high density aggregations (e.g. spawning aggregations and reef-associated fishes). The phenomenon of hyperstability may be more ubiquitous than previously thought if we consider the distribution of marine fishes as a function of population size and habitat suitability (MacCall, 1990). The basin model suggests that as abundance declines, populations will contract into areas of favorable habitat (MacCall, 1990; Rose and Kulka, 1999; Tremblay-Boyer et al., 2014), thereby creating the possibility for catch rates from targeted fisheries to remain high if fishing effort is focused on the areas of most suitable habitat.

In the pelagic environment, schooling behavior of fishes is a common life history trait that has been associated with predator avoidance (Godin, 1997; Zheng et al., 2005), increased forage opportunities (Pitcher et al., 1982; Milne et al., 2005), reproductive success (de Mitcheson and Colin, 2011), and energetic efficiency (Killen et al., 2012; Hemelrijk et al., 2015). Beginning around the 1960s, fishers began to exploit the schooling behavior of tunas, by using purse seines to harvest large volumes of fish thereby increasing their harvest efficiency (Miyake et al., 2004), but it wasn't until the 1980s that purse seine harvest contributed substantially to the regional tuna harvest (approximately 40% of the total tuna catch by the mid-1980s; Williams and Reid, 2019).

When CPUE is used as an input to stock assessment models, the traditional assumption is that the index is proportional to biomass; however, this assumption is rarely met when using CPUE from commercial fisheries (Harley et al., 2001). Effort, which is used to scale catch size, is not straightforward to quantify because it is the product of many different variables, some known, others potentially unknown. Examples of such variables include vessel power (Pascoe and Robinson, 1996), search technologies (Torres-Irineo et al., 2014), capture efficiency, but also skipper experience, management regimes, and socioeconomic drivers. In many cases, policy measures aimed at controlling fishing mortality through effort constraints (e.g. fleet capacity, vessel capacity, or temporal limitations), have been unsuccessful due to effort creep, i.e. increases in fishing efficiency through time (Pascoe and Coglan, 2000; Eigaard, 2009; Eigaard et al., 2014). Catch rates are typically standardized to control for factors that influence the efficiency of a unit of fishing effort; however, considerable variability may remain unaccounted for due to individual vessel effects or fishing activities, which may be unmeasurable. Effective effort is therefore, the combined effect of the measurable and unmeasurable (e.g. skipper effect, gear rigging, sophistication of electronics) factors that influence a vessel's efficiency (Hilborn, 1985; Marchal et al., 2007; Eigaard et al., 2014). These factors must be accounted for, to the extent possible, in a standardization procedure to ensure reliability of CPUE-based abundance indices.

The aim of this study is to address uncertainties related to CPUE for the tropical tuna purse seine fishery in the WCPO. Skipjack tuna *Katsuwonus pelamis* is the primary target of purse seine vessels in the WCPO, followed by yellowfin tuna *Thunnus albacares*, while small bigeye tuna *T. obesus* are occasionally harvested, often while fishing around fish aggregating devices (FADs). In 2018, 82% of skipjack and 56% of yellowfin harvested in the WCPO were landed by purse seiners (Williams and Reid, 2019). Historically, data from the pole-and-line fishery have been used to develop standardized indices of relative abundance for the skipjack stock assessments, but participation in this fishery has waned in recent decades due to the proliferation of the more efficient and profitable purse seine fishery, and therefore this fishery's ability to provide a reliable representation of the population dynamics across the WCPO has degraded. In the interest of using purse seine fishery data to inform trends in skipjack tuna abundance, we looked to observer collected data. Observers report set-level information on gear configurations, catch composition, crew demographics, and detailed accounts of vessel activities throughout the day; data predicted to be valuable in evaluating purse seine catch rates and developing an effective standardization methodology.

Standardization procedures for fishery catch rates are commonly performed using delta generalized linear models (GLMs), a.k.a. hurdle models. Delta-GLMs have long been viewed as the best-practice for CPUE standardization (Maunder and Punt, 2004; Lynch et al., 2012). However, with the development of accessible and efficient estimation algorithms (Thorson et al., 2015; Kristensen et al., 2016), alternative approaches are proving useful for this task. One of the major pitfalls of using traditional GLMs and delta-GLMs is the, often unreasonable, assumption of independence among observations in space and time (but also see Thorson, 2017). In simulation studies, delta models have performed well under a variety of conditions (Forrestal et al., 2019), but when sampling in space and time is unbalanced or clustered, potentially leading to unsampled strata, spatiotemporal models may outperform the more traditional GLMs (Ducharme-Barth et al., 2019). The focus of this study was to address some of the major limitations to purse seine CPUE standardization by: 1)

using observer data to more explicitly address effort creep and changes in catchability over time; 2) incorporating habitat variables expected to influence relative skipjack density; and 3) employing a spatiotemporal modeling framework to explicitly account for spatial and temporal correlation in catch rates. To complement the CPUE analyses, we have evaluated a suite of spatial distribution metrics (SDMs) as potential indicators of population dynamics, based on ecological theory. These analyses are intended to provide a base case standardization approach for use in regional stock assessment models. They may also provide the foundation for additional analyses related to CPUE standardization, such as: further exploration of changes in effective effort, understanding the effects of FAD density, addressing the influence of habitat suitability and oceanographic variation on catchability and abundance.

2 Methods

2.1 CPUE standardization

2.1.1 Catch and effort data

Operational (set-level) fishing effort and catch data were obtained from the Pacific Islands Regional Fisheries Observer Program data for the tuna purse seine fleets operating within the WCPO. As of 2010, 100% of tuna purse seine trips in the region were required to carry a fisheries observer, and therefore, the time series used for this analysis extended from 2010 through 2018. It should be noted that observer data made available to the Pacific Community (SPC) may be up to 20% less than the full coverage due to a suite of data issues (Williams et al., 2020). The skipjack stock assessment region, extends roughly from 50°N to 20°S and from 110°E to 150°W; however, the purse seine sector of the skipjack fishery primarily operates within the 2019 stock assessment Regions 6-8 (Figures 1 and 2); and therefore, those were the focal regions for these analyses.

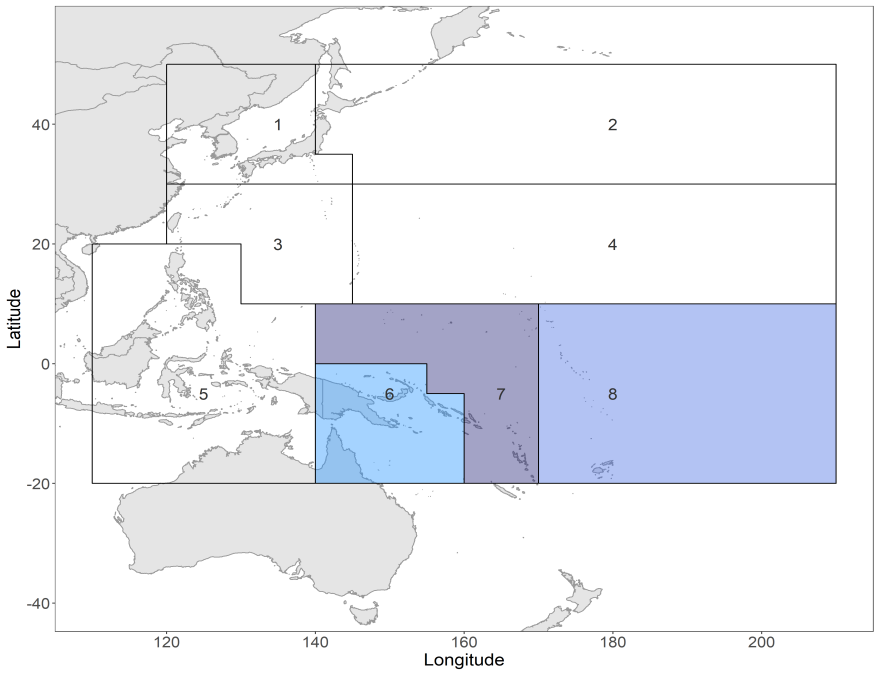

Figure 1: Regional stock assessment structure for skipjack, from the most recent assessment (2019). The regions highlighted in blue indicate the regions where the purse seine fishery is predominantly active, and therefore the focal regions for this analysis.

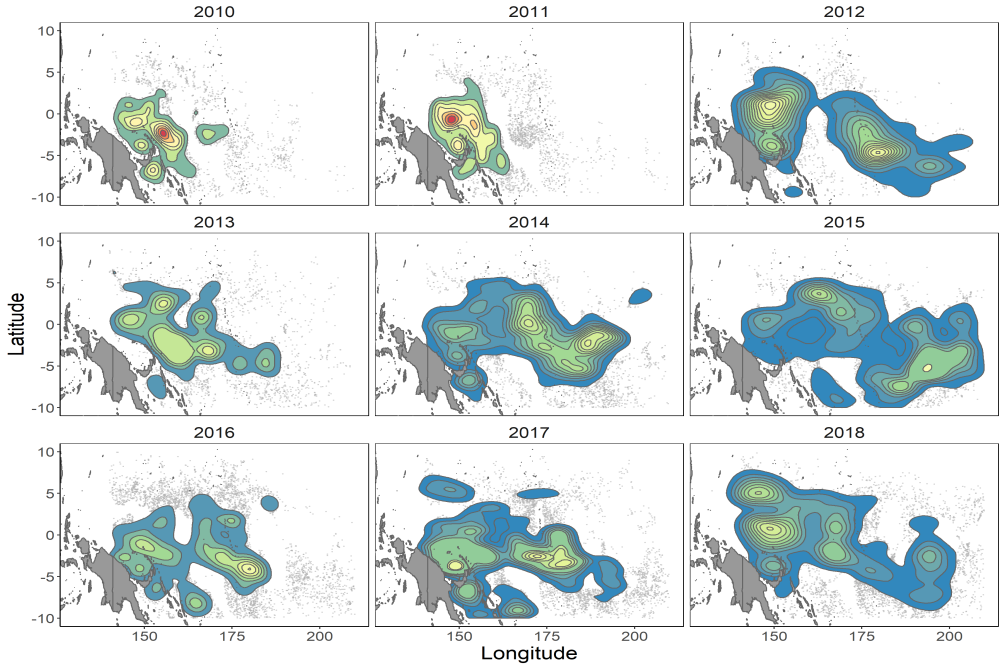

Figure 2: Observer reported purse seine effort (sets), highlighted with density contours, from 2010-2018. Individual sets are plotted as gray points.

Different fishing strategies are employed within the purse seine fleet, with the most salient difference distinguishing between associated and unassociated sets. Associated sets are those made in association with floating objects, either natural (e.g. logs, debris, whale sharks), or man-made (i.e. FADs). Historically, FADs were primarily anchored to the seabed; however, it is more common in the contemporary fishery for fishers to deploy and fish around drifting FADs (dFADs). Unassociated sets (UNA) are those made on free-schooling tuna unassociated with floating objects. During the time period of interest, dFAD and UNA sets compose the majority of the purse seine effort in the WCPFC-CA, and therefore were the focus of this analysis (Figure 3). It has been suggested that because of the substantial differences associated with fishing on FADs and unassociated schools, that the two should be analyzed separately (Hoyle et al., 2014). However, given that a vessel will commonly conduct both set types on the same trip, day, and in the same areas, and that both are targeting the same underlying stock, we chose to model them simultaneously with the inclusion of set type as a catchability covariate.

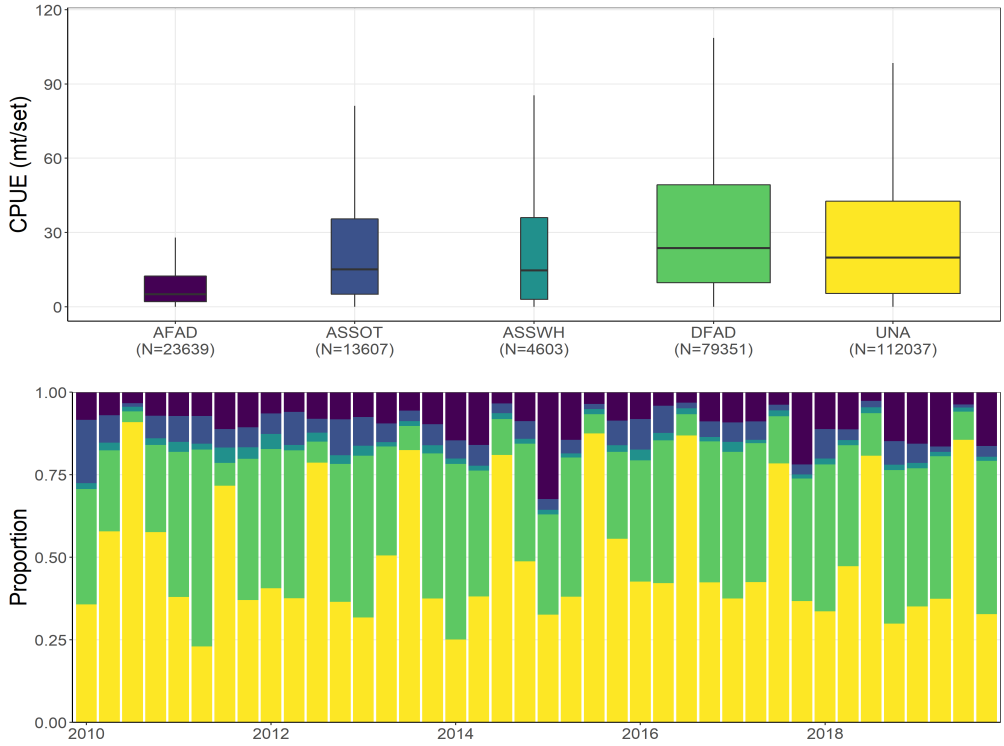

Figure 3: The distribution of skipjack catch rates by set type (mt/set; top), and the proportion of sets associated with each, in each year-quarter time step (bottom). Set types: AFAD = anchored FAD; ASSOT = associated other (e.g. logs, debris); ASSWH = associated with like whale; DFAD = drifting FAD; and UNA = unassociated free-school set. The boxplot widths are scaled by sample size (also noted in the x-axis labels). It should be noted, that observations have been filtered in these figures to remove failed sets and sets with extreme catch outliers (>99th quantile of tuna catches).

The full data set (n = 198,907 sets) was filtered to only include vessels between 50 and 80 m in length which were active in the fishery for approximately 20% of the time series of interest (observed

fishing activity in at least seven quarters between 2010 and 2018). To avoid a full exclusion of the vessels that had only recently entered the fishery, we included vessels that entered the fishery in 2017 or later if they had been active for at least four quarters (∼50% of the most recent two years of the time series). The vessel length criteria was imposed because when the Vessel Day Scheme (VDS), an effort-based management framework, was implemented in 2008, a fishing day differential was imposed based on vessel length (Dunn et al., 2006; Parties to the Nauru Agreement, 2016). Vessels within the 50-80 m range were charged one vessel day for one fishing day, while larger vessels were charged 1.5 vessel days per calendar day of fishing, and smaller vessels 0.5 days. Over the past decade, many of the largest vessels have left the fishery, leaving a fleet that is dominated by the 50-80 m size class. Focusing on this size class of vessels will help ensure the indicator is robust to future change in industry structure.

Sets, were identified as 'failed' sets if the total tuna catch was less than one mt, and removed from the data set as they were not expected to be representative of local density. In addition, extreme outlier catches (total tuna catch ≥99th quantile; 241 mt/set) were also removed. Lastly, records were removed if any data values were missing. The resulting filtered data set (n = 101,724) was used for the CPUE standardization. For a detailed description of the number of observations removed at each step of the data filtering process, refer to Table 1.

Filtering criteria	Removal %	Removal #
Vessel participation (>20% of time series; ∼7 quarters)	11%	21,094
Vessels between 50 and 80 m	15%	30,500
Removal of failed sets (total tuna catch) < 1 mt	2%	3,191
Extreme catch outliers (>99th quantile)	1%	1,442
Remove records with missing data	21%	40,956

Table 1: Summary of data filtering criteria employed. Note that some observations would have been excluded based on multiple selection criteria; the numbers removed are based on sequential filtering, and therefore may be an underestimate of observations relating to each criteria.

2.1.2 Model covariates

The R package *VAST* (Thorson et al., 2015) was used as the modeling framework. This modeling approach makes a distinction between covariates that affect catchability, and therefore are 'standardized' out of the estimated indices, and density covariates, which influence the abundance estimates. Density covariates may be of particular importance when extrapolating to unsampled areas; however, if true relationships are lacking, this model feature has the potential to introduce bias.

The purse seine fishery, like most industrial fisheries, has demonstrated the ability to continually evolve and adapt to changes in the resource as well as to management measures in an effort to maximize catch rates. Such changes, within an effort-based management framework, can undermine management and conservation objectives because catch rates may remain high as the

underlying stock declines, due to efficiency gains, or changes in effective effort over time (effort creep). Effective effort is not often directly measurable as it represents the combined effect of many different factors, with variable importance and trends through time. However, at this point, an effective multivariate or composite index which maps reliably to catchability, has not been developed.

Therefore, we selected a suite of vessel, gear, and strategy-based characteristics (i.e. set type, vessel length, gross registered tonnage, well capacity, skiff horsepower, net length, net depth, and a species composition cluster variable) to capture variability associated with effort creep, some of which were highly correlated (Figure 4). A k-means clustering algorithm was used to assign a species composition variable to each set, based on the proportion of each of the three main tuna species harvested in this fishery (skipjack, yellowfin, and bigeye). Two cluster groupings were selected, which were largely associated with skipjack dominated and yellowfin dominated sets (the two primary species harvested in this fishery). This species composition variable was predicted to be important given that this is a multi-species fishery, and a set dominated by yellowfin may skew our perception of the skipjack stock, if this variable is unaccounted for. From this set of potential covariates, we selected a subset hypothesized to represent catchability differences among the fleet, over time (Table 2).

In addition, we recognize the importance of oceanographic conditions (Table 2) in influencing the distribution and local abundance of tunas (e.g. Howell and Kobayashi, 2006; Bigelow and Maunder, 2007; Langley et al., 2009; Young et al., 2011). Temperature is often identified as one of the most salient drivers of marine fish distribution and abundance; however for tunas, it is well established that tuna aggregations often form along convergence zones where cold, saline waters merge with warmer waters to create prey hotspots (Fiedler and Bernard, 1987; Lehodey et al., 1997; Arrizabalaga et al., 2015; Lumban-Gaol et al., 2015). We compiled a suite of metrics relating to variability in oceanographic conditions, predicted to influence catch rates. After assessing the correlation among the metrics (Figure 4), we selected thermocline depth and ENSO to include in the model evaluations. Thermocline depth was predicted to influence catch rates due to the vertical compression of the upper mixed layer, and the associated vulnerability to a surface gear such as purse seines. Whereas, the ENSO effect was predicted to have a spatially-varying effect on density due to changes in sea surface temperature, and the location of the important east-west convergence zone. Lastly, moon phase was evaluated as it has been shown to influence catch rates in other tuna species (e.g. bigeye tuna), due to occupancy of deeper nighttime depths during the full moon as opposed to lesser illuminated phases (Evans et al., 2008). Variability in vertical aggregation due to moon phase was predicted to be of particular importance to FAD sets made during the early hours of the day, typically pre-dawn (Harley et al., 2009). Oceanographic data were obtained from the Global Ocean Data Assimilation System (GODAS), NOAA's high resolution sea surface temperature data (Banzon et al., 2019); and the E.U.'s Copernicus Marine Service, available monthly at 1/12° spatial resolution.

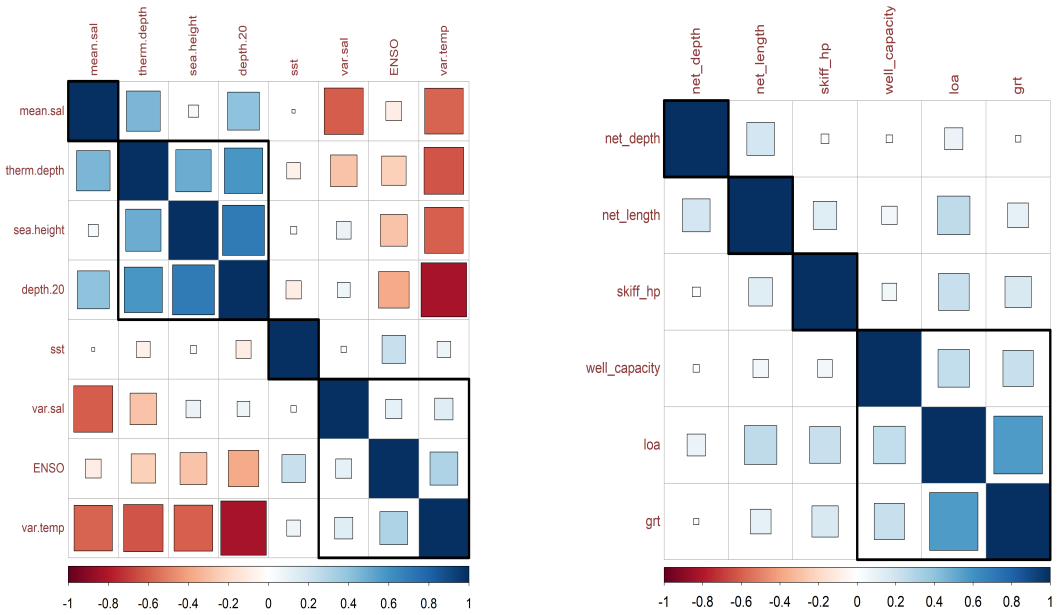

Figure 4: Hierarchical cluster correlation plots of the oceanographic and vessel characteristics variables considered for inclusion as catchability and density covariates in the model. Variables in the oceanographic data set (left) include: mean salinity in the upper 200 m of the water column (mean.sal); thermocline depth (therm.depth; m); sea surface height anomalies (sea.height; m), depth of the 20 degree isotherm (depth.20; m), sea surface temperature (sst, °C), variability in salinity in the upper 200 m of the water column (var.sal), ENSO, and variability in temperature in the upper 200 m. For the vessel-based characteristics we evaluated net depth (m), net length (m), skiff horsepower, well capacity (mt), vessel length (loa; m), and gross registered tonnage (grt).

Variable	Description
Catchability covariates	
Year-quarter	Categorical: temporal variable related to inter-annual changes in abundance
Vessel length	Continuous: overall vessel length (m)
Net length	Continuous: overall length of the purse seine net (m)
Species composition cluster	Categorical: Indicates whether the set's catch was dominated by skipjack or yellowfin
Set type	Categorical: unassociated or drifting FAD sets
Lunar phase	Categorical: new moon, first quarter, full, last quarter
Thermocline depth	Continuous: estimated depth of the thermocline from the Global Ocean Data Assimilation System (m)
Density covariate	
El Niño Southern Oscillation	Continuous: ENSO anomaly from Niño Region 4 (5N-5S, 160E-150W)

Table 2: Description of catchability and density covariates selected for evaluation in the spatiotemporal CPUE standardization models, after omitting highly correlated variables.

Exploratory data analyses demonstrated an increase in vessel and net length over time, with relatively consistent proportions of UNA sets and sets dominated by skipajck (Figure A.11). The relationship between skipjack catch rates (CPUE) and the vessel, gear, and strategy-based characteristics suggested: a positive, but variable, relationship between CPUE and vessel length; that DFAD sets tended to have slightly higher catch rates than UNA sets; and that skipjack dominated sets tended to produce larger catches, which is a natural construct of this variable. Non-linear relationships between skipjack catch rates and net length and thermocline depth were detected (Figure A.12), and therefore we evaluated the use of a zero-mean-constrained spline (Wood, 2015) to model these effects, such that the splines did not influence the model intercept (i.e. the year-quarter effect). Moon phase and ENSO showed little contrast in the raw CPUE data. These variables were retained for evaluation in the suite of candidate models because ENSO, in particular, was expected to have a variable effect across space (Yen et al., 2017), and therefore, the effect on CPUE may not be apparent in the aggregated data. Moon phase was assessed under a similar hypothesis, such that it may be influential when considered in combination with other explanatory variables.

2.1.3 Spatiotemporal model

We fit a suite of spatiotemporal delta generalized linear mixed models (GLMMs), using the VAST package in R (Thorson et al., 2015). Spatiotemporal models implicitly account for spatial and temporal autocorrelation in catch rates using smooth functions (Thorson et al., 2015), addressing one of the potential pitfalls of traditional delta-GLMs. Each model component was estimated using Gaussian Markov random fields, assuming geometric anisotropy (i.e. the degree of spatial autocorrelation can vary based on directionality of neighboring knots) to allow for density predictions based on aggregate impacts of the environment and biological factors, factors that may influence the distribution of a given species as well as the catchability (Thorson, 2019b). Spatial locations at which the effects were estimated (i.e. the knots; n=150) were uniformly distributed across the spatial domain. This knot configuration results in an estimated spatial effect for approximately every 3° x 3° spatial cell. Observed data points were assigned to the nearest knot for estimation (Figure A.14), and density predictions are made using bilinear interpolation, averaging across the neighboring knot predictions. The catch data were positively skewed with a high proportion of zeros, owing to sets composed of yellowfin or even bigeye tuna, as failed sets were removed from the data set. The probability of a positive catch was assumed to have a binomial error distribution, while we assumed a gamma error distribution for the magnitude of positive catches. For a detailed description of the model, see Appendix A.1.

Precise geographic position data at the set level were used for the model fitting, and an extrapolation grid of 1° x 1° grid cells corresponding to Regions 6-8 of the 2019 skipjack assessment were used for estimation of the regional indices. Eleven candidate models were run for evaluation and comparison.

2.2 Spatial distribution metrics

Spatial indicators and metrics of distribution have been employed for a range of research objectives including to assess ecosystem services (Syrbe and Walz, 2012), evaluate indicators of abundance for deep-sea stocks (Trenkel et al., 2013), detect biomass thresholds for marine fishes (Reuchlin-Hugenholtz et al., 2015), assess changes in catchability due to fishing strategies (Tidd et al., 2017), and for general surveillance of marine systems to inform management (Rufino et al., 2018). The development of reliable, generalizable spatial indicators for monitoring abundance trends is still lacking, however. We propose that such indicators can be employed as part of a 'dashboard' of tools that, when used together, could inform our understanding of population dynamics and complement information from CPUE-based abundance trends.

2.2.1 Data and metric calculation

Many different (potentially redundant) spatial indicators have been proposed and employed for different objectives, most of which can be grouped into three general categories: those relating to occupancy, aggregation, or quantity (Rufino et al., 2018). Here, we assessed indicators associated with each of the three categories of spatial distribution, using fisher-reported logsheet data, due to the relatively long time-series available (as compared to the shorter but more reliable observer data). We then compared the spatial distribution metrics (SDMs) to estimates of biomass from the most recent stock assessment (Vincent et al., 2019). Lastly, we evaluated inference from the SDMs (using logbook data) against the standardized CPUE indices from the purse seine fishery, using observer data (described in section 2.1.3).

Using fisher-reported logsheet data from 2000-2018, we aggregated catch and effort from the regions of purse seine activity (Regions 6-8; Figures 1 and 2) to 1° x 1° cells in each time step. Fishing effort is not randomly distributed throughout the region, as fishers selectively target regions of expected higher fish density. Following an approach laid out by Reuchlin-Hugenholtz et al. (2015), we evaluated the following SDMs: 1) area occupied (occupancy/range), 2) the minimum area containing 90% of the catch (aggregation); 3) Gini index of evenness (aggregation/evenness), and 4) proportion of sets that fall into four categories relating to zero, low, medium, or high catch levels (abundance). The SDM time series were then evaluated against biomass estimates from the stock assessment.

The distributional range of fish species can be an important indicator of range shifts as well as contraction or expansion in space. Area occupied (AO) is one measure of distributional range, and reflects the proportion of the total fished area where skipjack was detected, in a given year y.

$$AO_y = \frac{\sum_{s=1}^{S_y} \frac{x_{sy}^p}{x_{ys}} A_s}{\sum A_{ys}}$$

where x_{ys}^p is the number of sets in 1° cell s with positive catch, x_{ys} is the total number of sets per cell s, and A_{ys} is the area of cell s, whereas the denominator is the sum of the total fished area (all

cells fished, by set type, during the time period). It should be noted that the area of each cell was taken to equal to 110^2 km^2, a reasonable estimate for the equatorial region.

The minimum area containing 90% of the purse seine catches (D90) can be viewed as a metric of aggregation or concentration of the catches. This quantity was calculated, by set type, by first calculating the mean catch $\bar{C}_{ys}$ size for each 1° x 1° cell s in each year y, weighting each cell by the area associated, and then dividing by the summation of the area weighted average catches across all fished cells.

$$\overline{WC}_{ys} = \frac{\bar{C}_{ys} * \frac{A_{ys}}{\sum_{s=1}^{S_y} A_{ys}}}{\sum_{s=1}^{S_y} \left(\bar{C}_{ys} * \frac{A_{ys}}{\sum_{s=1}^{S_y} A_{ys}} \right)}$$

Here A, refers to the area of each cell, which was assumed to be 110^2 km^2 for all cells throughout the region. The weighted catches $\overline{WC}_{ys}$ were summed cumulatively, ordered by catch magnitude, until 90% of the catch was achieved. The area associated with the minimum cells to produce 90% of the total catch was then summed to yield the D90 metric. Given that all cells were of approximately the same size, this equation can be simplified as follows.

$$\overline{WC}_{ys} = \frac{\bar{C}_{ys}}{\sum_{s=1}^{S_y} \bar{C}_{ys}}$$

As an alternative metric of aggregation, the Gini index was calculated, to quantify patchiness of catches, but also to describe how evenly biomass (using catch as a proxy) is spread across the region of interest. Gini index values range from 0 to 1, with increasing values suggesting greater spatial concentration. Aggregate catch in each cell is compared to the cumulative sum of all catches (C), in a given year. The index is estimated by the area between the Lorenz curve (L_x) and the 1:1 diagonal (even distribution of biomass). The Lorenz curve represents the cumulative proportion of biomass relative to the cumulative proportion of area sampled multiplied by 2, and was calculated using the R package *OasisR* (Tivadar, 2019).

$$G_y = 1 - 2 \int_0^1 L_x dx$$

Lastly, we classified each set into one of four catch categories, based on magnitude: zero, low, medium, and high. This classification was set type (UNA vs dFAD) specific, and was determined using quantiles of the data. The quantiles were also species specific, such that a zero catch might indicate no landed skipjack, but it's possible the set produced a catch dominated by yellowfin. This metric indicates the proportion of sets associated with four catch density categories: zero, low ($>$0 and $\leq$ 33.3%), the medium ($>$33.3% and $\leq$66.7%), and the high ($>$66.7%). It should be noted that sets with zeros (no skipjack catch) were removed prior to calculating the quantiles for the non-zero catches.

2.2.2 Correlation with abundance

To evaluate the relationship between the estimated SDMs and skipjack biomass B, we performed a series of linear regressions. Non-linear regressions (not shown here) were evaluated, but were outperformed by simple linear regression models.

$$B_y = \beta_0 + \beta_1 \cdot \text{SDM}_y$$

SDMs and biomass estimates were all standardized (Z_m) by scaling to the maximum time series value, prior to analysis, to facilitate comparison among different indicators.

$$Z_m = \frac{m}{m_{max}}$$

Identifying significant and reliable relationships between SDMs and biomass may be useful as alternative metrics to assess stock status and to compare with inference from CPUE analyses.

2.3 Demographics

Demographic trends can be valuable when monitoring population dynamics, because general patterns associated with compensatory responses have been detected, especially with respect to fishing. For example, over time, truncation of the age and size-structure (Berkeley et al., 2004b), increased variability in recruitment (Berkeley et al., 2004a; Anderson et al., 2008), and maturation at younger ages and smaller sizes (DeCelles and Vidal, 2020) have all been associated with overexploitation. Therefore, demographic information could be used to detect signs of overexploitation even if biomass estimates remain high. Such changes are important, because it has been shown that populations may become less resilient to adverse conditions or variability in the environment when they lose the buffering capacity potentially associated with a broad reproducing age structure (Ottersen et al., 2006; Hidalgo et al., 2011) or phenotypic and genetic diversity (Hsieh et al., 2010; Ciannelli et al., 2013). Unfortunately, we do not have rich data sets on changes in growth or maturation over a long time series, but we do have information on length frequency data collected by observers. Observers typically collect length measurements (fork length, cm) from five fish per brail on purse seine sets. These data were summarized, by set type, to qualitatively assess changes to the size distribution, as harvested by the purse seine fishery.

3 Results

3.1 CPUE standardization

The standardized biomass indices were relatively stable over the time series, in the three regions we evaluated (Figure 5). All of the candidate models, excepting one, converged on a solution;

and all demonstrated very similar trends in biomass (although the magnitude varied) over the time series. Using AIC-based selection criteria, convergence statistics, and general interest in interpretability (e.g. ensuring retention of a set type covariate), from the 11 models investigated (Table 3) we identified model 10 as the preferred model. The model selection process is not of great importance here as all models largely suggested similar patterns in relative abundance. The preferred model included set type, species composition cluster, and vessel length as catchability covariates, with ENSO as a proxy that influences habitat suitability. Seasonal variability is notable in the indices, due in part to the seasonal FAD closure and reallocation of effort during those months. The biomass in Region 8 is predicted to be substantially greater than in Regions 6 and 7, largely due to the larger associated area.

Model	Covariates	AIC	Δ AIC
1	MP + CL + VL + ST + s(NL) + s(TD) + svc(ENSO)	X	
2	MP + VL + ST + s(NL) + s(TD) + svc(ENSO)	898471.2	41302.8
3	VL + ST + s(NL) + s(TD) + svc(ENSO)	898591.0	41422.6
4	ST + s(NL) + s(TD) + svc(ENSO)	898558.4	41390.0
5	ST + s(TD) + svc(ENSO)	898586.8	41418.4
6	VL + ST + s(TD)	898553.3	41384.9
7	CL + VL + ST + s(NL) + s(TD) + svc(ENSO)	898558.4	41390.0
8	CL + VL + ST + s(NL) + s(TD)	857179.0	10.6
9	CL + VL + ST + s(TD) + svc(ENSO)	857176.2	7.8
10	**CL + VL + ST + svc(ENSO)**	857168.4	0
11		900835.2	43666.8

Table 3: Suite of model configurations evaluated, with corresponding AIC values used for model selection. Covariates are indicated by the following: MP = moon phase; CL = species composition cluster; VL = vessel length; ST = set type (FAD versus free-school); NL = net length; TD = thermocline depth; and ENSO = El Niño Southern Oscillation index. An s() around the covariate abbreviation indicates it was fitted as a spline, while svc() indicates a spatially varying coefficient. Model 10, in bold font, was identified as the preferred model. An X in the AIC column indicates the model failed to converge, and therefore was not considered as a viable candidate model.

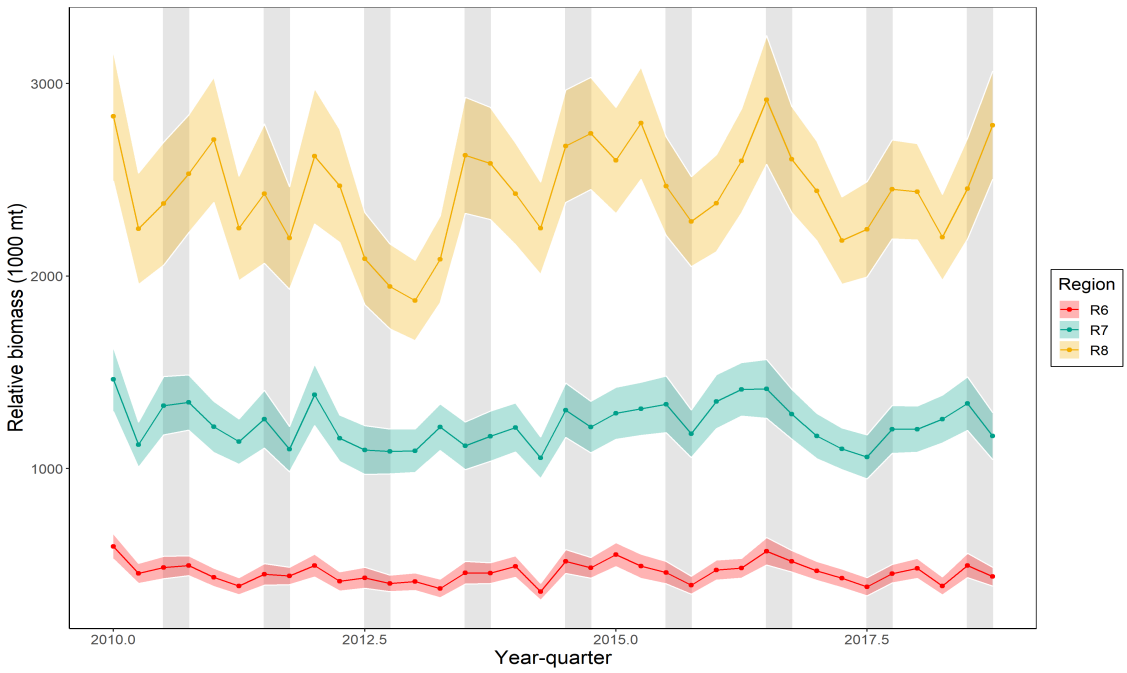

Figure 5: Area-weighted relative biomass indices (1000 mt) for Regions 6, 7, and 8 of the 2019 skipjack tuna stock assessment. Annual three-month FAD closure periods indicted with gray rectangles.[2]

The relative biomass indices from the candidate models varied, largely due to covariates included; however the mean-standardized abundance indices were nearly indistinguishable (Figure 6). In all regions, abundance estimates fluctuated around the mean throughout the time series, but lacked clear directional trends. The standardized indices smoothed through some of the variability associated with the nominal index, but otherwise, the general patterns through time were comparable.

[2]The FAD closure period is not all-inclusive, as there are exemptions during the main 3-month closure, and from 2013-2017, there was an additional closure throughout the month of October for vessels flagged to a CCM[3]without specific FAD fishing limits (WCPFC, 2012).

[3]CCM = Cooperating Members, Cooperating non-members and Participating Territories of the WCPFC

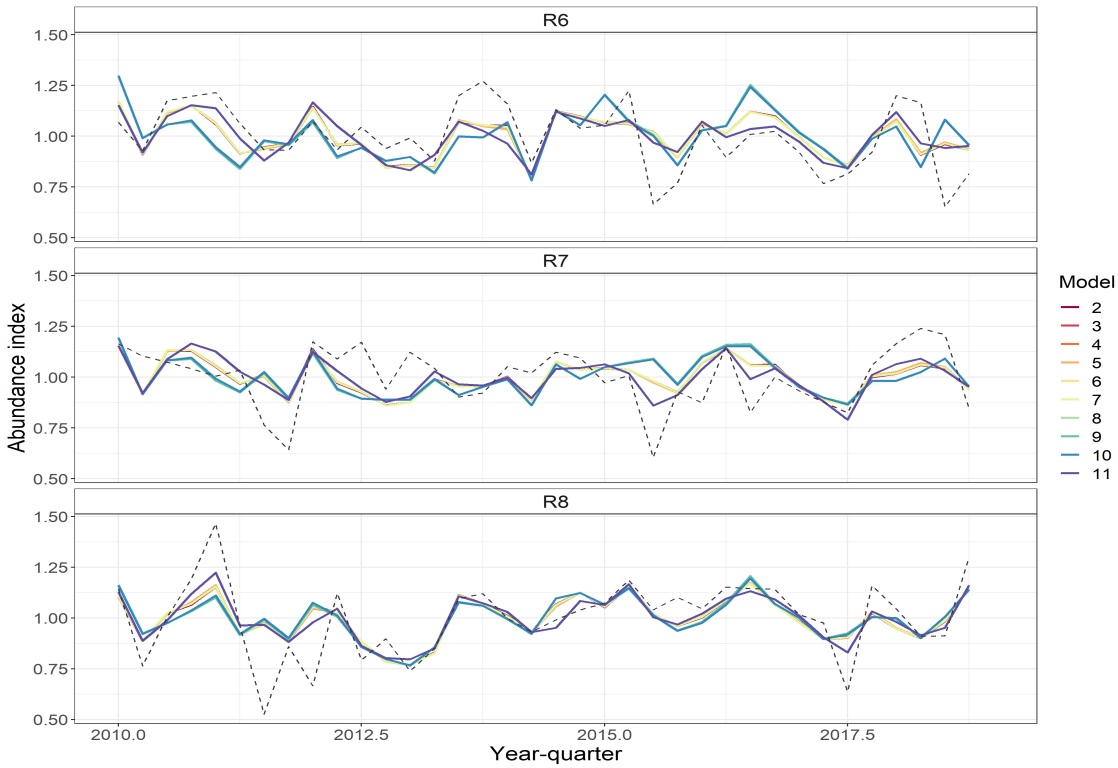

Figure 6: Comparison of mean-standardized candidate models, along with the nominal CPUE (gray dashed line), by region from 2010-2018. The value of 1 on the y-axis represents the time series mean.

The influence metrics (Bentley et al., 2012) for the covariates included, were minimal over the time series (Figure 7). Vessel length showed a positive trend, suggesting the index would be higher in recent years without the inclusion of vessel length in the model. The influence metrics for set type were negligible, and for the species composition variable, the influence was variable through time, but largely stable, lacking a directional trend. The large peaks in the cluster variable influence are associated with time periods of relatively low skipjack catch, and relatively high yellowfin to skipjack ratios.

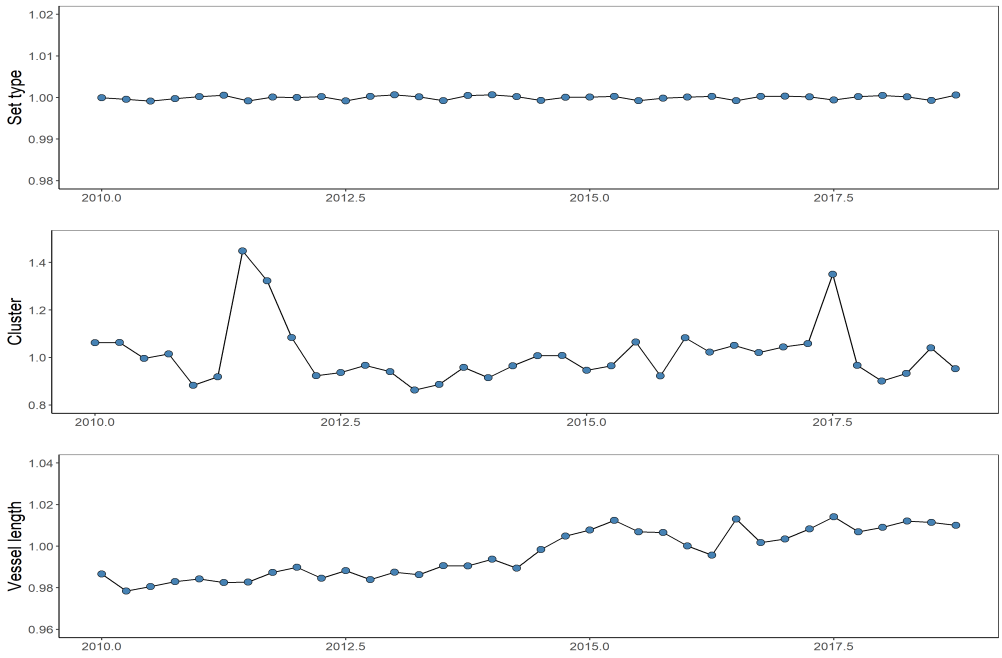

Figure 7: Influence plots for covariates included in the preferred model.

Residual patterns and the q-q plot suggested a reasonable model fit without any discernible patterns suggesting violation of distributional assumptions (Figures A.15 and A.16) . Although the standardized indices are fairly stable throughout the time series, there are seasonal and inter-annual fluctuations in estimated relative density across the spatial domain (Figure A.17), due in part to oscillations in the ENSO phase. For example, during much of 2010, 2015, 2016, and in the most recent time period, high density areas were shifted more towards the eastern equatorial WCPO, due to El Niño conditions, while during the La Niña phase, high density areas were more towards the west. However, it should be noted that the El Niño phase has dominated for much of the past two decades.

3.2 SDMs

The spatial distribution metrics were calculated across the entire study region (i.e. Regions 6-8 of the skipjack stock assessment; Figure 1) as they were predicted to reflect overall stock dynamics unrelated to the regional construct used for the assessment model. We did however, estimate the proposed metrics for dFAD and free-school (UNA) sets separately, to try to determine whether the set type influenced our perception of the spatial distribution of the stock.

Area occupied showed a positive trend for both dFAD and UNA sets, with a steeper trend observed for dFAD sets (Figure 8). The minimum area containing 90% of the purse seine catches (D90), for both dFAD and UNA sets showed a sharp increase over the time series, suggesting a broader spatial distribution associated with skipjack catches. The Gini index was fairly stable at about 0.5 for both

set types, while the proportion of 'high' catches showed opposite trends for dFAD and UNA sets. The proportion of high catches from dFAD sets demonstrated a slight positive trend, while UNA sets have shown a slight decline over time.

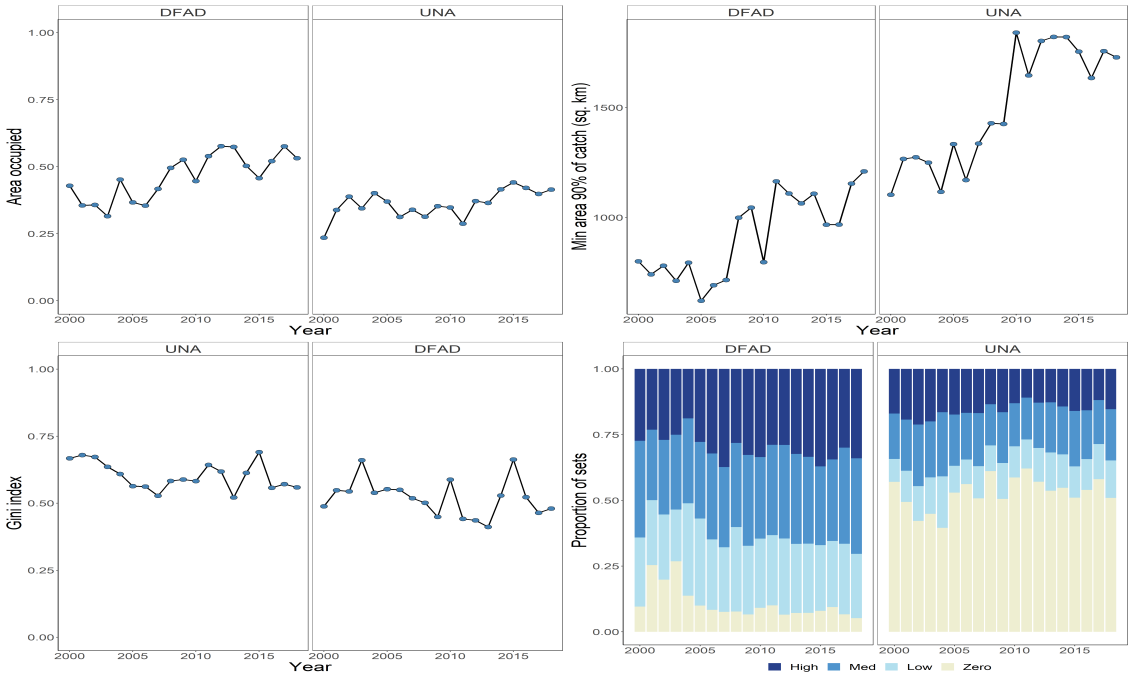

Figure 8: Time series of annual SDMs, by set type, from 2000-2018.

Figure 9 illustrates the regressions for which the SDMs were significant ($p \leq 0.05$) in explaining variability in skipjack biomass. Area occupied, minimum area to produce 90% of the catch, and proportion of high catches were all positively related to biomass, as predicted. Therefore, as biomass increases, the stock may be more dispersed through its range, with a greater area supporting catches, and the probability of relatively high catches increasing. The Gini index did not explain significant variability in biomass, which is not unexpected, given that the index was relatively flat at about 0.5 throughout the time series. The relationships between the SDMs and biomass, combined with the SDM time series, generally suggested that indicators positively associated with biomass have been increasing over the recent time series.

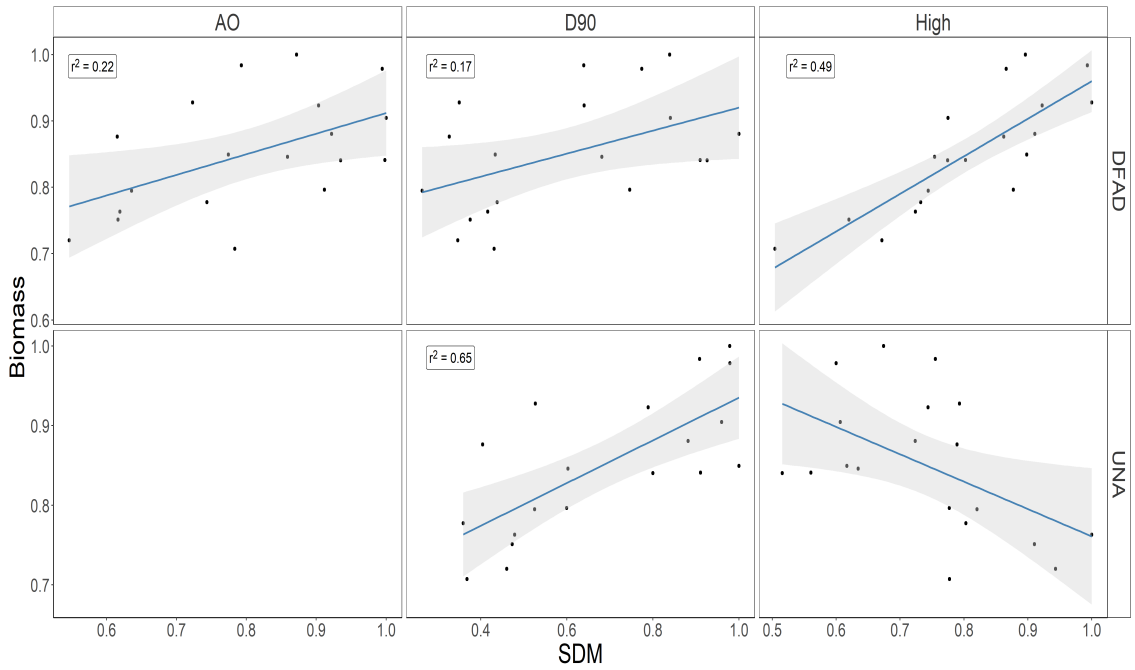

Figure 9: Significant linear regressions (slope parameters with $p \leq 0.05$) predicting biomass from SDMs, by set type, with the annual estimates plotted as points. AO = area occupied; D90 = minimum density to achieve 90% of the catch; and High = proportion of high catch sets. R-squared values from the regressions are noted in the figures.

SDMs may be useful as proxy indicators, relating to biomass trends, but they may also play a role with respect to climate change. Here, we have evaluated changes in the center of gravity of the distribution and inertia (variability around the center of gravity) from 2000-2018, based on fishery catch data. There was some evidence that the center of gravity has trended towards the south and east (Figure A.18) in recent years, potentially due to the persistence of positive El Niño conditions. Figures A.19 and A.20 illustrate the center of gravity and inertia of skipjack from UNA and dFAD sets. In general, the two show similar patterns, although dFAD sets have a tendency for greater inertia. There is also notable inter-annual variability in the equatorial spread of the distribution, again, potentially related to the distribution of the western warm pool. It should be noted that these analyses were also performed using effort (sets) as the response variable as opposed to catch, with very similar results and interpretation. The one difference between the two approaches was that the proportion of high drifting FAD effort was an insignificant predictor of biomass, whereas the proportion of high free-school sets showed a positive relationship with biomass.

3.3 Length frequencies

The length frequency data (Figure 10) suggest that for skipjack the mode of the length distribution varied year to year, perhaps in response to relatively strong cohorts moving through the population, but there is no obvious unidirectional trend in the size structure. As expected, UNA sets tends to

catch larger skipjack, while dFAD sets tend to catch the smaller size classes; however, the respective set-specific size structures are relatively consistent throughout the time series.

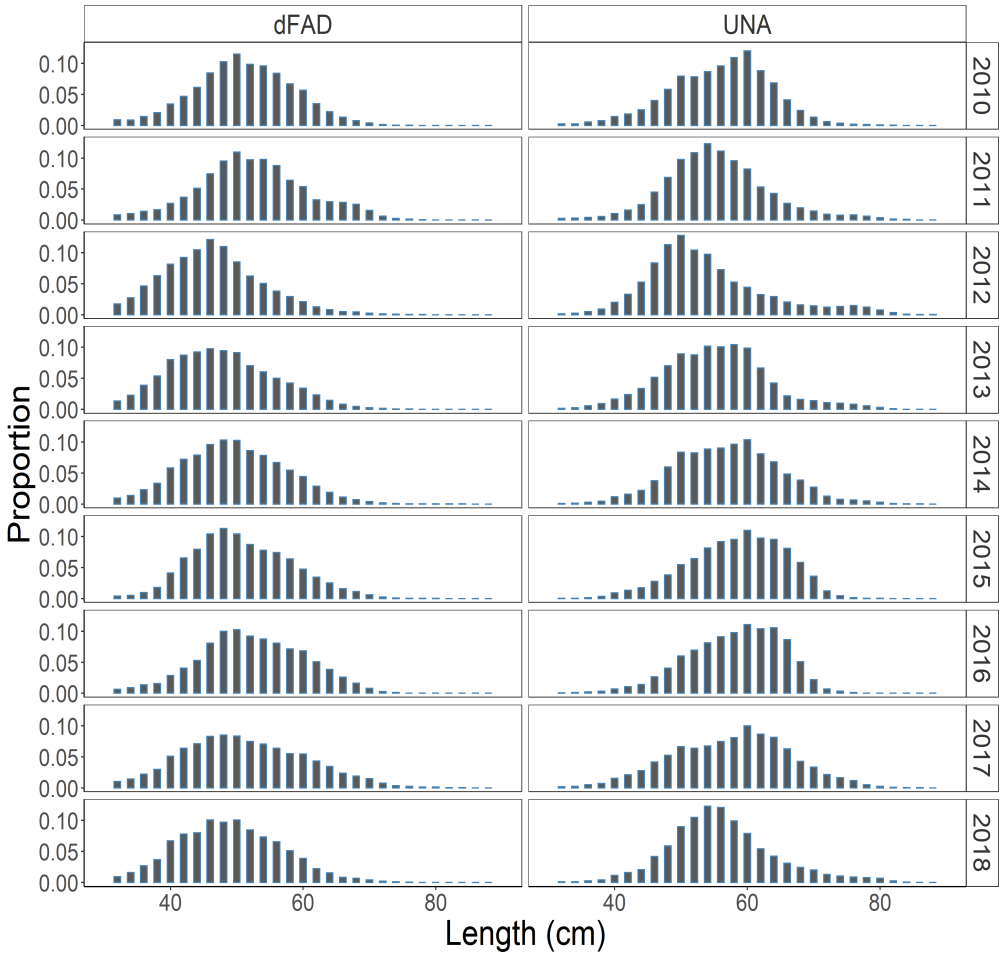

Figure 10: Observer collected length frequency (fork length, cm) data for skipjack tuna from dFAD and UNA purse seine sets, from 2010-2018.

4 Discussion

This analysis represents one of the first broad-scale efforts to standardize skipjack CPUE from the purse seine fishery in the WCPO, for use in future stock assessment models. The standardized indices suggest that biomass has been relatively stable since 2010, inference that is generally supported by the spatial distribution metrics. The spatiotemporal modeling framework employed offers a powerful unified framework for standardizing catch rates, which effectively controls for autocorrelation in space and time which could arise due to tuna behavior, variability in the environment, or impacts of management measures (e.g. FAD closure period). One of the potential limitations, however, is that the spatial and spatio-temporal terms in the model tend to absorb a substantial portion of the variability, variability that might otherwise be explained by model

covariates. This implicit explanatory power of variability in the data may be valuable for effectively estimating trends in biomass, potentially at the cost of disentangling the main drivers of those trends. For example, in the models we have evaluated, the mean-standardized indices were relatively insensitive to the catchability and density covariates included in the model, a situation similarly observed in an analysis of yellowfin purse seine catch rates (Vidal and Hamer, 2020); however the model without any covariates (Model 11) did deviate slightly from the models informed by covariates on catchability (Figure 6).

The spatial distribution metrics and length data were included here to provide a 'dashboard' of information with which to evaluate skipjack trends through time. Standardized catch rates can be highly influential in assessment models, especially when there's a paucity of reliable, alternative or complementary, data sources (e.g. fishery-independent surveys, demographic information). By incorporating multiple sources of information, we may be better able to buffer against uncertainty and make more informed decisions related to long-term sustainable management. The relationships between the SDMs and biomass were noisy; however, the general trends observed aligned with expectations regarding changes in distribution of the population with changes in overall biomass, and were inconsistent with a decreasing biomass trend. Specifically, area occupied and minimum area to capture 90% of the catch (D90) demonstrated a positive relationship with biomass and both have generally increased over the time series, albeit less so over the shorter-term time series associated with the CPUE indices. There was also a notable increase in the minimum area to capture 90% of the catch around the implementation of the VDS, potentially due to the distribution of VDS fishing days among PNA EEZs (and thus a distribution in effort) or perhaps, due to information from echo-sounder FAD buoys. The proportion of high catch sets is interesting in that it increased for dFAD sets while decreased for UNA sets. It should be noted that over the recent decade, high catch free-school sets have generally increased, excepting 2017, which appeared to be a bit of an anomaly. In general, the SDMs have suggested a relatively stable skipjack biomass over the time series from 2010 to 2018, corroborating the inference from the CPUE-based indices.

We have interpreted the SDMs largely within the framing of the basin model (MacCall, 1990); however, consideration needs to be given to the ecological-trap hypothesis (Marsac et al., 2000). Given that FAD-associated SDMs and biomass were significant predictors of biomass, continued investigations into the behavior of tunas around FADs and changes in catch rates with variable FAD densities remains a priority. If FADs are effectively working to attract schooling tunas, even in less favorable habitats, our perception of the relationship between the SDMs considered and biomass may be skewed.

Hyperstability remains an important concerns with using purse seine catch rates as indices of abundance, potentially masking population declines. Here, we have included covariates to explain vessel and gear-based characteristics predicted to influence catchability over time, as well as a set type covariate (UNA versus dFAD) to explain differences in catchability associated with the two main purse seine fishing strategies. In addition, this modeling framework has the flexibility to include habitat covariates, or proxies, predicted to influence density, a potentially valuable feature for estimating density in unsampled strata. Although we have selected variables to capture facets of effort creep, we acknowledge that the complexity associated with changes in effective effort likely exceeds that which we have captured here. There have been great strides made in the

sophistication of information technologies used for fishing, and such advancements are ongoing. For example, vessels are now using dual-frequency echo-sounder FAD buoys (Escalle et al., 2020) to better differentiate species composition associated with individual FAD buoys. This information may be combined with information from oceanographic sensing tools, communication with other vessels, and from land-based analysts, all of which may influence decision making and ultimately catch rates and spatial patterns of fishing effort. Continually improving our understanding of the factors that influence these decisions and the relative importance of each is an ongoing task as long as the assessment and monitoring of tuna stocks is reliant on fishery-dependent information. SPC is involved with several ongoing projects to better understand these dynamics, including the development of a fisher survey; leveraging information from vessel monitoring system (VMS) data; and statistical analyses of observer and logbook data aimed at partitioning variability in catch rates using data-driven modeling approaches (Wichman et al., 2020).

The model presented here was intended to provide a 'base case' model for standardization of skipjack CPUE from the purse seine fishery, and to serve as a platform from which to further evaluate important questions related to catch rates and factors influencing them. For example:

- How does FAD density affect catch rates?;
- Can FAD-mounted echo-sounder data improve abundance estimates by providing estimates of presence/absence of tunas in unfished areas (e.g. Grüss and Thorson, 2019)?;
- Can a variance-partitioning framework be used to better quantify the effect of effort creep in the purse seine fishery?; and
- How can VMS data be used to reevaluate our definition of purse seine effort based on fishing and searching behaviors?

At this stage, we invite SC16 to take note of the proposed approach to provide a purse seine CPUE-based abundance index to inform the next skipjack tuna stock assessment and to lend support for the proposed research to advance these analyses. Specifically, supporting continued efforts to: improve monitoring of tuna populations through statistical analysis; to address effort creep (e.g. Wichman et al., 2020); to collect detailed data on FAD activity and encourage data sharing, including data collected by FAD-mounted electronics; and lastly, support increased biological sampling/processing efforts, including an analysis of changes in maturation schedules over time (and see also Macdonald et al., 2020 for proposed sampling approaches). These research efforts will serve to improve these analyses and enhance our understanding of tuna dynamics.

5 Acknowledgments

We thank the Pacific-European Union Marine Partnership (PEUMP) Programme for funding TV's position, under KRA 1.5 'Improved modelling of relative abundance using catch per unit effort', which has facilitated these analyses; Jim Thorson et al. for the development of the VAST package

as well as for hosting a workshop to help participants understand the modeling tool better and utilize it more effectively; Steven Hare for his valuable comments on an earlier version of this document. We would also like to sincerely thank the Pacific Islands Regional Fishery Observers for the difficult and dangerous work they do to provide valuable information for the assessment and management of tropical tuna stocks.

6 References

Anderson, C. N. K., Hsieh, C.-h., Sandin, S. A., Hewitt, R., Hollowed, A., Beddington, J., May, R. M., and Sugihara, G. (2008). Why fishing magnifies fluctuations in fish abundance. *Nature*, 452(7189):835–839.

Arrizabalaga, H., Dufour, F., Kell, L., Merino, G., Ibaibarriaga, L., Chust, G., Irigoien, X., Santiago, J., Murua, H., Fraile, I., et al. (2015). Global habitat preferences of commercially valuable tuna. *Deep Sea Research Part II: Topical Studies in Oceanography*, 113:102–112.

Banzon, V., Reynolds, R., and National Center for Atmospheric Research Staff (Eds) (2019). The Climate Data Guide: SST data: NOAA High-resolution (0.25x0.25) Blended Analysis of Daily SST and Ice, OISSTv2. https://climatedataguide.ucar.edu/climate-data/sst-data-noaa-high-resolution-025x025-blended-analysis-daily-sst-and-ice-oisstv2. Accessed: 2019-10-10.

Bentley, N., Kendrick, T. H., Starr, P. J., and Breen, P. A. (2012). Influence plots and metrics: tools for better understanding fisheries catch-per-unit-effort standardizations. *ICES Journal of Marine Science*, 69(1):84–88.

Berkeley, S. A., Chapman, C., and Sogard, S. M. (2004a). Maternal age as a determinant of larval growth and survival in a marine fish, *Sebastes melanops*. *Ecology*, 85(5):1258–1264.

Berkeley, S. A., Hixon, M. A., Larson, R. J., and Love, M. S. (2004b). Fisheries sustainability via protection of age structure and spatial distribution of fish populations. *Fisheries*, 29(8):23–32.

Bigelow, K., Garvilles, E., Bayate, D. E., and Cecilio, A. (2019). Relative abundance of skipjack tuna for the purse seine fishery operating in the Philippines Moro Gulf (Region 12) and High Seas Pocket #1. *Western and Central Pacific Fisheries Commission 15th Regular Session*.

Bigelow, K. A. and Maunder, M. N. (2007). Does habitat or depth influence catch rates of pelagic species? *Canadian Journal of Fisheries and Aquatic Sciences*, 64(11):1581–1594.

Cashion, T., Al-Abdulrazzak, D., Belhabib, D., Derrick, B., Divovich, E., Moutopoulos, D. K., Noël, S.-L., Palomares, M. L. D., Teh, L. C., Zeller, D., et al. (2018). Reconstructing global marine fishing gear use: Catches and landed values by gear type and sector. *Fisheries Research*, 206:57–64.

Ciannelli, L., Fisher, J. A., Skern-Mauritzen, M., Hunsicker, M. E., Hidalgo, M., Frank, K. T., and Bailey, K. M. (2013). Theory, consequences and evidence of eroding population spatial structure in harvested marine fishes: a review. *Marine Ecology Progress Series*, 480:227–243.

de Mitcheson, Y. S. and Colin, P. L. (2011). *Reef fish spawning aggregations: biology, research and management*, volume 35. Springer Science & Business Media.

DeCelles, G. R. and Vidal, T. (2020). Long-term changes in the maturation and growth of Cape Cod/Gulf of Maine yellowtail flounder *Limanda ferruginea*. *Marine Ecology Progress Series*, 633:169–180.

Ducharme-Barth, N., Vincent, M., Pilling, G., and Hampton, J. (2019). Simulation analysis of pole and line CPUE standardization approaches for skipjack tuna in the WCPO. *Western and Central Pacific Fisheries Commission 15th Regular Session*.

Dunn, S., Rodwell, L., and Joseph, G. (2006). The Palau Arrangement for the management of the Western Pacific purse seine fishery-management scheme (Vessel Day Scheme). In *Sharing the Fish Conference, Perth*.

Eigaard, O. R. (2009). A bottom-up approach to technological development and its management implications in a commercial fishery. *ICES Journal of Marine Science*, 66(5):916–927.

Eigaard, O. R., Marchal, P., Gislason, H., and Rijnsdorp, A. D. (2014). Technological development and fisheries management. *Reviews in Fisheries Science & Aquaculture*, 22(2):156–174.

Erisman, B. E., Allen, L. G., Claisse, J. T., Pondella, D. J., Miller, E. F., and Murray, J. H. (2011). The illusion of plenty: hyperstability masks collapses in two recreational fisheries that target fish spawning aggregations. *Canadian Journal of Fisheries and Aquatic Sciences*, 68(10):1705–1716.

Escalle, L., Muller, B., Hare, S., Hamer, P., Pilling, G., and PNAO (2020). Report on analyses of the 2016/2020 PNA FAD tracking programme. *Western and Central Pacific Fisheries Commission 16th Regular Session*, WCPFC-SC16-2020/ MI-IP-14.

Evans, K., Langley, A., Clear, N. P., Williams, P., Patterson, T., Sibert, J., Hampton, J., and Gunn, J. S. (2008). Behaviour and habitat preferences of bigeye tuna (*Thunnus obesus*) and their influence on longline fishery catches in the western Coral Sea. *Canadian Journal of Fisheries and Aquatic Sciences*, 65(11):2427–2443.

Fiedler, P. C. and Bernard, H. J. (1987). Tuna aggregation and feeding near fronts observed in satellite imagery. *Continental shelf research*, 7(8):871–881.

Forrestal, F. C., Schirripa, M., Goodyear, C. P., Arrizabalaga, H., Babcock, E. A., Coelho, R., Ingram, W., Lauretta, M., Ortiz, M., Sharma, R., et al. (2019). Testing robustness of CPUE standardization and inclusion of environmental variables with simulated longline catch datasets. *Fisheries Research*, 210:1–13.

Godin, J.-G. (1997). Evading predators. *Behavioural ecology of teleost fishes*.

Grüss, A. and Thorson, J. T. (2019). Developing spatio-temporal models using multiple data types for evaluating population trends and habitat usage. *ICES Journal of Marine Science*, 76(6):1748–1761.

Hamilton, R. J., Almany, G. R., Stevens, D., Bode, M., Pita, J., Peterson, N. A., and Choat, J. H. (2016). Hyperstability masks declines in bumphead parrotfish (*Bolbometopon muricatum*) populations. *Coral Reefs*, 35(3):751–763.

Harley, S., Williams, P., and Hampton, J. (2009). Analysis of purse seine set times for different school associations: a further tool to assist in compliance with FAD closures? *Western and Central Pacific Fisheries Commission 5th Regular Session*, WCPFC-SC5-2009/ ST-WP-07, Port Vila, Vanuatu.

Harley, S. J., Myers, R. A., and Dunn, A. (2001). Is catch-per-unit-effort proportional to abundance? *Canadian Journal of Fisheries and Aquatic Sciences*, 58(9):1760–1772.

Hemelrijk, C., Reid, D., Hildenbrandt, H., and Padding, J. (2015). The increased efficiency of fish swimming in a school. *Fish and Fisheries*, 16(3):511–521.

Hidalgo, M., Rouyer, T., Molinero, J. C., Massutí, E., Moranta, J., Guijarro, B., and Stenseth, N. C. (2011). Synergistic effects of fishing-induced demographic changes and climate variation on fish population dynamics. *Marine Ecology Progress Series*, 426:1–12.

Hilborn, R. (1985). Fleet dynamics and individual variation: why some people catch more fish than others. *Canadian Journal of Fisheries and Aquatic Sciences*, 42(1):2–13.

Hilborn, R. and Walters, C. J. (1992). Quantitative fisheries stock assessment: choice, dynamics and uncertainty. *Reviews in Fish Biology and Fisheries*, 2(2):177–178.

Howell, E. A. and Kobayashi, D. R. (2006). El Niño effects in the Palmyra Atoll region: oceanographic changes and bigeye tuna (*Thunnus obesus*) catch rate variability. *Fisheries Oceanography*, 15(6):477–489.

Hoyle, S. D., Langley, A. D., and Campbell, R. A. (2014). Recommended approaches for standardizing CPUE data from pelagic fisheries. *Western and Central Pacific Fisheries Commission 10th Regular Session*, WCPFC-SC10-2014/SA-IP-10.

Hsieh, C.-h., Yamauchi, A., Nakazawa, T., and Wang, W.-F. (2010). Fishing effects on age and spatial structures undermine population stability of fishes. *Aquatic Sciences*, 72(2):165–178.

Killen, S. S., Marras, S., Steffensen, J. F., and McKenzie, D. J. (2012). Aerobic capacity influences the spatial position of individuals within fish schools. *Proceedings of the Royal Society B: Biological Sciences*, 279(1727):357–364.

Kristensen, K., Nielsen, A., Berg, C. W., Skaug, H., and Bell, B. (2016). TMB: automatic differentiation and Laplace approximation. *Journal of Statitical Software*.

Langley, A., Briand, K., Kirby, D. S., and Murtugudde, R. (2009). Influence of oceanographic variability on recruitment of yellowfin tuna (*Thunnus albacares*) in the western and central Pacific Ocean. *Canadian Journal of Fisheries and Aquatic Sciences*, 66(9):1462–1477.

Lehodey, P., Bertignac, M., Hampton, J., Lewis, A., and Picaut, J. (1997). El Niño Southern Oscillation and tuna in the western Pacific. *Nature*, 389(6652):715–718.

Lumban-Gaol, J., Leben, R. R., Vignudelli, S., Mahapatra, K., Okada, Y., Nababan, B., Mei-Ling, M., Amri, K., Arhatin, R. E., and Syahdan, M. (2015). Variability of satellite-derived sea surface height anomaly, and its relationship with Bigeye tuna (*Thunnus obesus*) catch in the Eastern Indian Ocean. *European Journal of Remote Sensing*, 48(1):465–477.

Lynch, P. D., Shertzer, K. W., and Latour, R. J. (2012). Performance of methods used to estimate indices of abundance for highly migratory species. *Fisheries Research*, 125:27–39.

MacCall, A. D. (1990). *Dynamic geography of marine fish populations*. Washington Sea Grant Program Seattle, WA.

Macdonald, J., Roupsard, F., Leroy, B., Sanchez, C., and Hosken, M. (2020). Additional options for implementing WCPO Biological Sampling . *Western and Central Pacific Fisheries Commission 16th Regular Session*, WCPFC-SC16-2020/ RP-P35b-01.

Marchal, P., Andersen, B., Caillart, B., Eigaard, O., Guyader, O., Hovgaard, H., Iriondo, A., Le Fur, F., Sacchi, J., and Santurtún, M. (2007). Impact of technological creep on fishing effort and fishing mortality, for a selection of European fleets. *ICES Journal of Marine Science*, 64(1):192–209.

Marsac, F., Fonteneau, A., and Ménard, F. (2000). Drifting FADs used in tuna fisheries: an ecological trap? In *Pêche thonière et dispositifs de concentration de poissons, Caribbean-Martinique, 15-19 Oct 1999*.

Maunder, M. N. and Punt, A. E. (2004). Standardizing catch and effort data: a review of recent approaches. *Fisheries Research*, 70(2):141–159.

Milne, S., Shuter, B., and Sprules, W. (2005). The schooling and foraging ecology of lake herring (*Coregonus artedi*) in Lake Opeongo, Ontario, Canada. *Canadian Journal of Fisheries and Aquatic Sciences*, 62(6):1210–1218.

Miyake, M. P., Miyabe, N., and Nakano, H. (2004). *Historical trends of tuna catches in the world*. Number 467. Food & Agriculture Org.

Ottersen, G., Hjermann, D. Ø., and Stenseth, N. C. (2006). Changes in spawning stock structure strengthen the link between climate and recruitment in a heavily fished cod (*Gadus morhua*) stock. *Fisheries Oceanography*, 15(3):230–243.

Parties to the Nauru Agreement (2016). Palau Arrangement for the management of the Western Pacific fishery as amended - management scheme (purse seine Vessel Day Scheme). Technical report.

Pascoe, S. and Coglan, L. (2000). Implications of differences in technical efficiency of fishing boats for capacity measurement and reduction. *Marine Policy*, 24(4):301–307.

Pascoe, S. and Robinson, C. (1996). Measuring changes in technical efficiency over time using catch and stock information. *Fisheries Research*, 28(3):305–319.

Pitcher, T., Magurran, A., and Winfield, I. (1982). Fish in larger shoals find food faster. *Behavioral Ecology and Sociobiology*, 10(2):149–151.

Reuchlin-Hugenholtz, E., Shackell, N. L., and Hutchings, J. A. (2015). The potential for spatial distribution indices to signal thresholds in marine fish biomass. *PLOS ONE*, 10(3):e0120500.

Rose, G. and Kulka, D. (1999). Hyperaggregation of fish and fisheries: how catch-per-unit-effort increased as the northern cod (*Gadus morhua*) declined. *Canadian Journal of Fisheries and Aquatic Sciences*, 56(S1):118–127.

Rufino, M. M., Bez, N., and Brind'Amour, A. (2018). Integrating spatial indicators in the surveillance of exploited marine ecosystems. *PLOS ONE*, 13(11):e0207538.

Syrbe, R.-U. and Walz, U. (2012). Spatial indicators for the assessment of ecosystem services: providing, benefiting and connecting areas and landscape metrics. *Ecological indicators*, 21:80–88.

Thorson, J. T. (2017). Three problems with the conventional delta-model for biomass sampling data, and a computationally efficient alternative. *Canadian Journal of Fisheries and Aquatic Sciences*, 75(9):1369–1382.

Thorson, J. T. (2019a). Forecast skill for predicting distribution shifts: a retrospective experiment for marine fishes in the Eastern Bering Sea. *Fish and Fisheries*, 20(1):159–173.

Thorson, J. T. (2019b). Guidance for decisions using the Vector Autoregressive Spatio-Temporal (VAST) package in stock, ecosystem, habitat and climate assessments. *Fisheries Research*, 210:143–161.

Thorson, J. T. (2019c). Measuring the impact of oceanographic indices on species distribution shifts: The spatially varying effect of cold-pool extent in the eastern Bering Sea. *Limnology and Oceanography*, 64(6):2632–2645.

Thorson, J. T. and Haltuch, M. A. (2019). Spatiotemporal analysis of compositional data: increased precision and improved workflow using model-based inputs to stock assessment. *Canadian Journal of Fisheries and Aquatic Sciences*, 76(3):401–414.

Thorson, J. T., Pinsky, M. L., and Ward, E. J. (2016). Model-based inference for estimating shifts in species distribution, area occupied and centre of gravity. *Methods in Ecology and Evolution*, 7(8):990–1002.

Thorson, J. T., Shelton, A. O., Ward, E. J., and Skaug, H. J. (2015). Geostatistical delta-generalized linear mixed models improve precision for estimated abundance indices for west coast groundfishes. *ICES Journal of Marine Science: Journal du Conseil*, page fsu243.

Tidd, A., Brouwer, S., and Pilling, G. (2017). Shooting fish in a barrel? Assessing fisher–driven changes in catchability within tropical tuna purse seine fleets. *Fish and fisheries*, 18(5):808–820.

Tivadar, M. (2019). OasisR: An R package to bring some order to the world of segregation measurement. *Journal of Statistical Software*, 89(7):1–39.

Torres-Irineo, E., Gaertner, D., Chassot, E., and Dreyfus-León, M. (2014). Changes in fishing power and fishing strategies driven by new technologies: The case of tropical tuna purse seiners in the eastern Atlantic Ocean. *Fisheries Research*, 155:10–19.

Tremblay-Boyer, L., Harley, S., and Pilling, G. (2014). Relationship between abundance and range size in longline target species. *Western and Central Pacific Fisheries Commission 10th Regular Session*, WCPFC-SC10-2014/ MI-WP-06.

Trenkel, V. M., Beecham, J. A., Blanchard, J. L., Edwards, C. T., and Lorance, P. (2013). Testing CPUE-derived spatial occupancy as an indicator for stock abundance: application to deep-sea stocks. *Aquatic Living Resources*, 26(4):319–332.

Vidal, T. and Hamer, P. (2020). Developing yellowfin tuna recruitment indices from drifting FAD purse seine catch and effort data. *Western and Central Pacific Fisheries Commission 16th Regular Session*, WCPFC-SC16-2020/ SA-IP-08.

Vidal, T., Pilling, G., Tremblay-Boyer, L., and Usu, T. (2019). Standardized CPUE for skipjack *Katsuwonus pelamis* from the Papua New Guinea archipelagic purse seine fishery. *Western and Central Pacific Fisheries Commission 15th Regular Session*, WCPFC-SC15-2019/ SA-IP-05.

Vincent, M., Pilling, G., and Hampton, J. (2019). Stock assessment of skipjack tuna in the western and central Pacific Ocean. *Western and Central Pacific Fisheries Commission 15th Regular Session*, WCPFC-SC15-2019/ SA-WP-05.

Western and Central Pacific Fisheries Commission (WCPFC) (2012). Conservation and management measure for bigeye, yellowfin and skipjack tuna in the Western and Central Pacific Ocean. 9th regular session of the Western and Central Pacific Fisheries Commission. *Manila, Philippines*, pages 2–6.

Wichman, W., Vidal, T., and Hamer, P. (2020). Purse seine effort creep research plan. *Western and Central Pacific Fisheries Commission 16th Regular Session*, WCPFC-SC16-2020/ MI-IP-16.

Williams, P., Panizza, A., Falasi, C., and Loganimoce, E. (2020). Status of observer data management. *Western and Central Pacific Fisheries Commission 16th Regular Session*, WCPFC-SC16-2020/ ST-IP-02.

Williams, P. and Reid, C. (2019). Overview of Tuna Fisheries in the Western and Central Pacific Ocean, including Economic Conditions – 2018. *Western and Central Pacific Fisheries Commission 15th Regular Session*.

Wood, S. (2015). Package 'mgcv'. *R package version*, 1:29.

Yen, K.-W., Wang, G., and Lu, H.-J. (2017). Evaluating habitat suitability and relative abundance of skipjack (*Katsuwonus pelamis*) in the Western and Central Pacific during various El Niño events. *Ocean & coastal management*, 139:153–160.

Young, J., Hobday, A., Campbell, R., Kloser, R., Bonham, P., Clementson, L., and Lansdell, M. (2011). The biological oceanography of the East Australian Current and surrounding waters in relation to tuna and billfish catches off eastern Australia. *Deep Sea Research Part II: Topical Studies in Oceanography*, 58(5):720–733.

Zheng, M., Kashimori, Y., Hoshino, O., Fujita, K., and Kambara, T. (2005). Behavior pattern (innate action) of individuals in fish schools generating efficient collective evasion from predation. *Journal of theoretical biology*, 235(2):153–167.

A Appendix

A.1 Model specification

The linear predictors for encounter probability and magnitude of positive catch rates (model component, encounter probability or positive catch rate, is denoted as m) are modeled for knot s and time step t, with the respective link functions (i.e. logit for the encounter probability and log link for the positive catch rates), as

$$m_i = \beta_m(t_i) + \eta_m(v_i) + \omega_m(s_i) + \epsilon_m(s_i, t) + \sum_{k=1}^{\eta_k} \lambda_k Q(i,k)$$

where β is the year-quarter effect, $\eta(v_i)$ is a random vessel effect, $\omega(s_i)$ is the spatial effect, $\epsilon(s_i, t)$ is the spatio-temporal effect, and λ_k represents the fixed catchability effects for $Q(i,k)$ catchability covariates. The spatial variation terms $\omega(s_i)$ are assumed to come from a Gaussian random field, and treated as random effects, assuming a Matern covariance matrix to account for spatial autocorrelation.

$$\omega_m \sim \text{MVN}(0, \sigma^2_{\omega m}\mathbf{R_m})$$

Separate decorrelation rates $\mathbf{R_m}$ (related to the anisotropy) were estimated for each model component (Thorson, 2019a). The spatio-temporal random effects $\epsilon(s_i, t)$ account for the interaction between time and the model spatial structure.

A random vessel effect was included to account for overdispersion and is assumed to follow a Gaussian distribution with a mean of zero and estimated variance parameter. Density at each knot in each time period $d(s,t)$ was estimated by obtaining the product of the back-transformed linear predictors, after dropping the catchability terms. The abundance index is then calculated as the sum of the area-weighted densities

$$I(t) = \sum_{s=1}^{N_s} a(s) d(s,t)$$

where $a(s)$ is the area associated with knot s. Regional indices were calculated as the area in each region associated with each knot, multiplied by the respective density; standard errors associated with the indices are calculated internally in Template Model Builder (TMB) using the inverse Hessian and the delta method (Thorson et al., 2016).

In addition, we evaluated the inclusion of a spatially-varying coefficient (SVC; γ_s) to explain spatial variation in density associated with ENSO (Thorson and Haltuch, 2019),

$$m_i = \beta_m(t_i) + \eta_m(v_i) + \omega_m(s_i) + \phi_m(s_i, t) + \sum_{k=1}^{\eta_k} \lambda_k Q(i,k) + \gamma_s E + \epsilon_i$$

where

$$\gamma_s = \gamma_0 + \gamma_x(s)$$

$$\gamma_x \sim MVN(0, \Sigma)$$

and γ_o is the average slope across space, and γ_x is the zero-mean function representing spatial variation in the response to ENSO. During warm phases (El Niño conditions) this convergence zone is pushed farther to the east, while in La Niña phases, the convergence zone is more to the west. As a result, the direction and magnitude of the effect of the ENSO phase on skipjack density throughout the spatial domain of interest, may be highly variable (Yen et al., 2017). To address this source of variability, instead of estimating a single slope parameter associated with the ENSO covariate, SVCs were used to estimate a spatially varying random effect (Thorson, 2019c), thereby allowing a range of density responses across space, in response to fluctuations in the ENSO index.

A.2 Supplemental figures

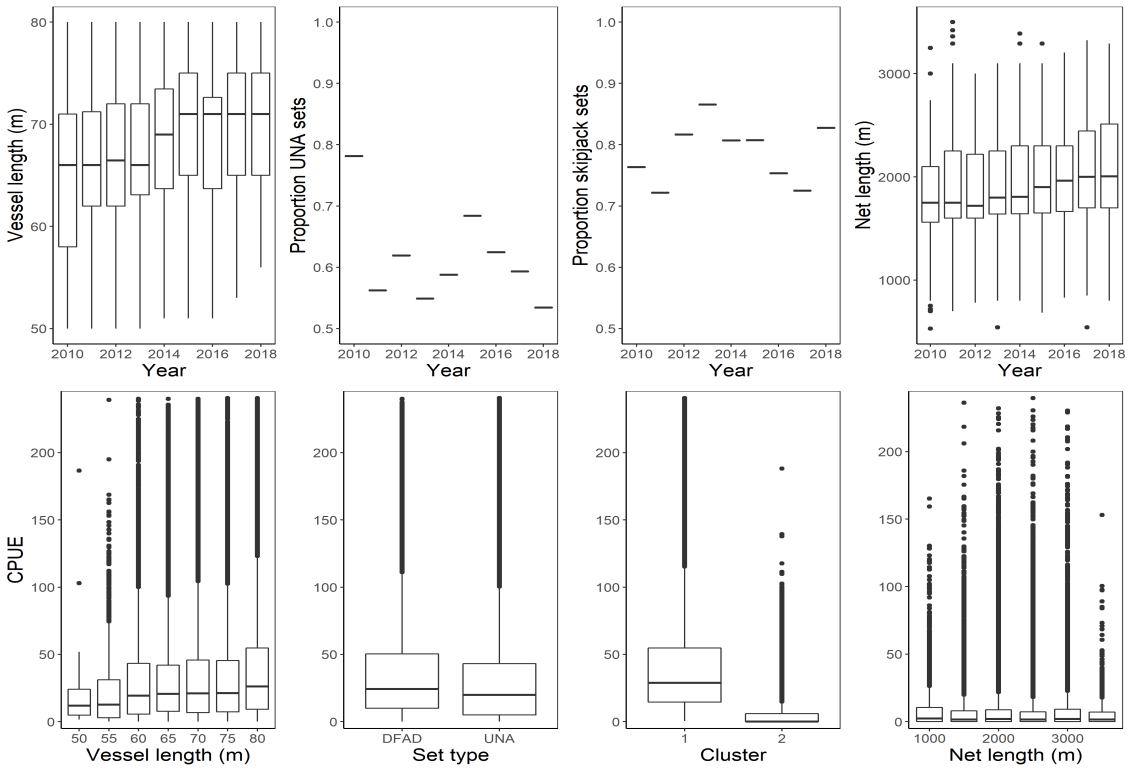

Figure A.11: Distribution of observed vessel length, set type (drifting FAD (dFAD) or free-school (UNA) set), species composition cluster (1=set was dominated by skipjack; 2 = set was dominated by yellowfin), and net length (top), as well as the relationship between these variables and skipjack CPUE (mt/set; bottom), from the filtered data set.

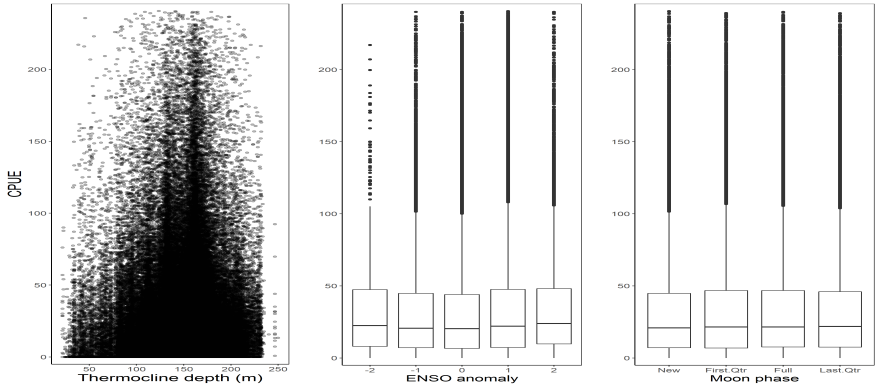

Figure A.12: Skipjack CPUE (mt/set) plotted against the environmental covariates, thermocline depth, ENSO, and moon phase, included in the candidate model suite, from the filtered data set.

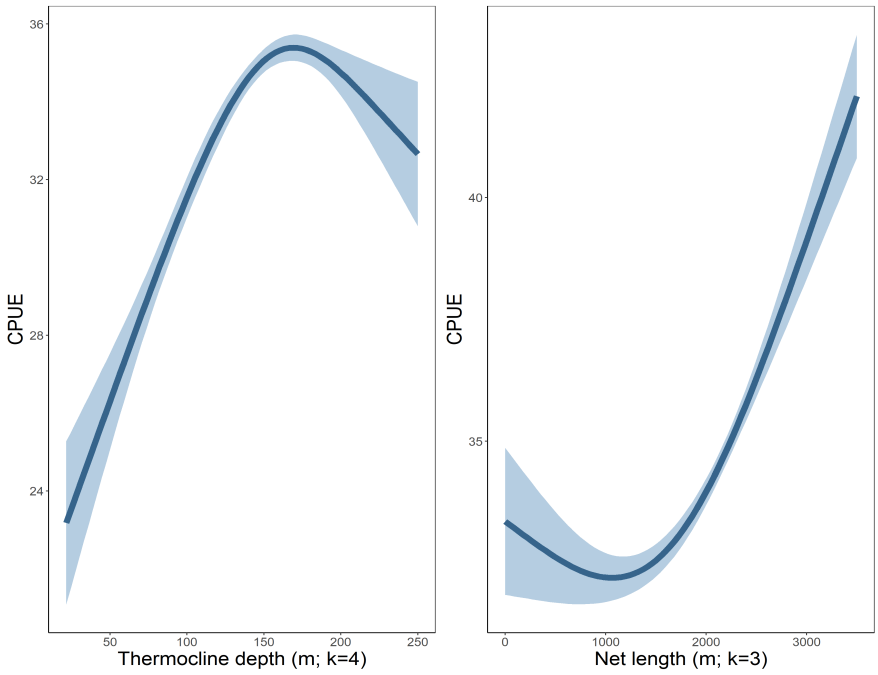

Figure A.13: Illustration of the nonlinear relationship between skipjack CPUE and the catchability covariates, thermocline depth and net length, fitted using spline with k knots.

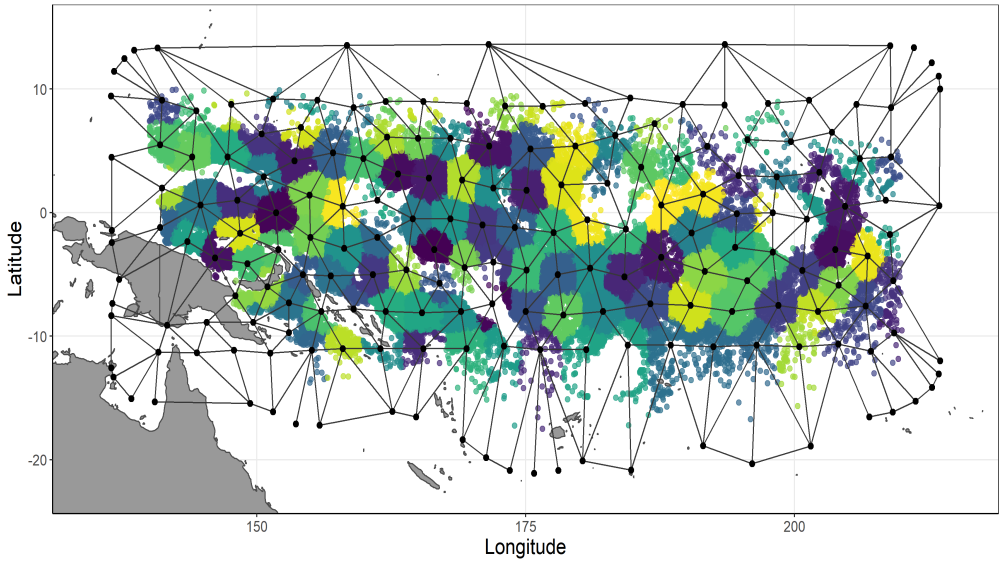

Figure A.14: Spatial knot placement (uniform; n=150) and mesh configuration used in the spatiotemporal estimation model. Observation-level data points are color-coded based on the nearest knot.

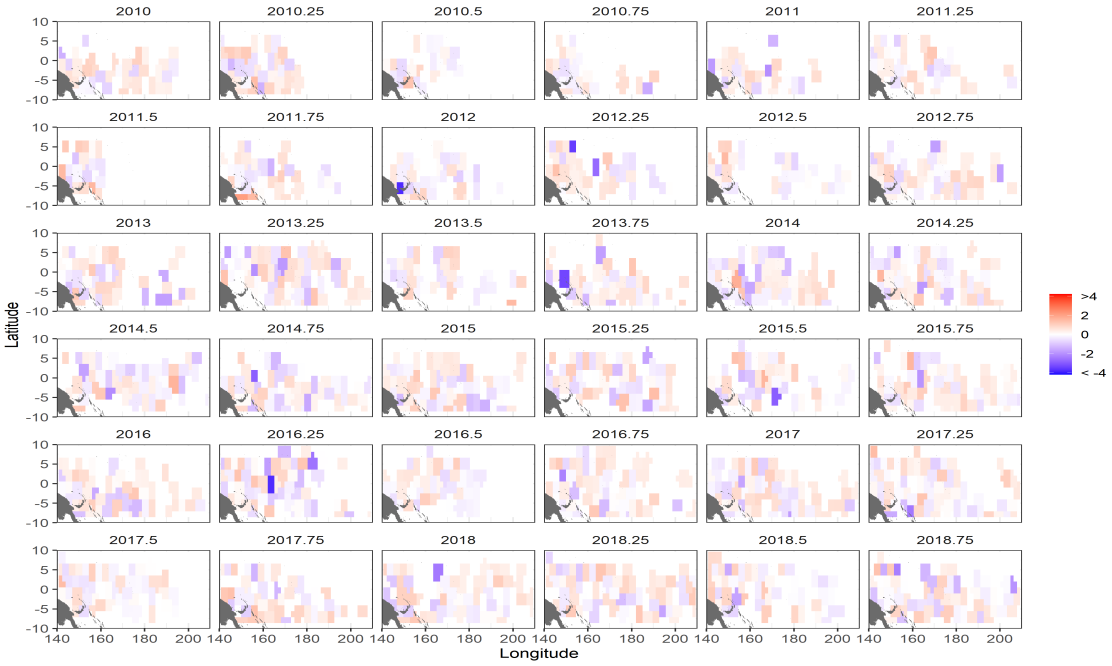

Figure A.15: Mean Pearson residuals, by (1° x 1°) extrapolation grid cell, for the encounter probability model component.

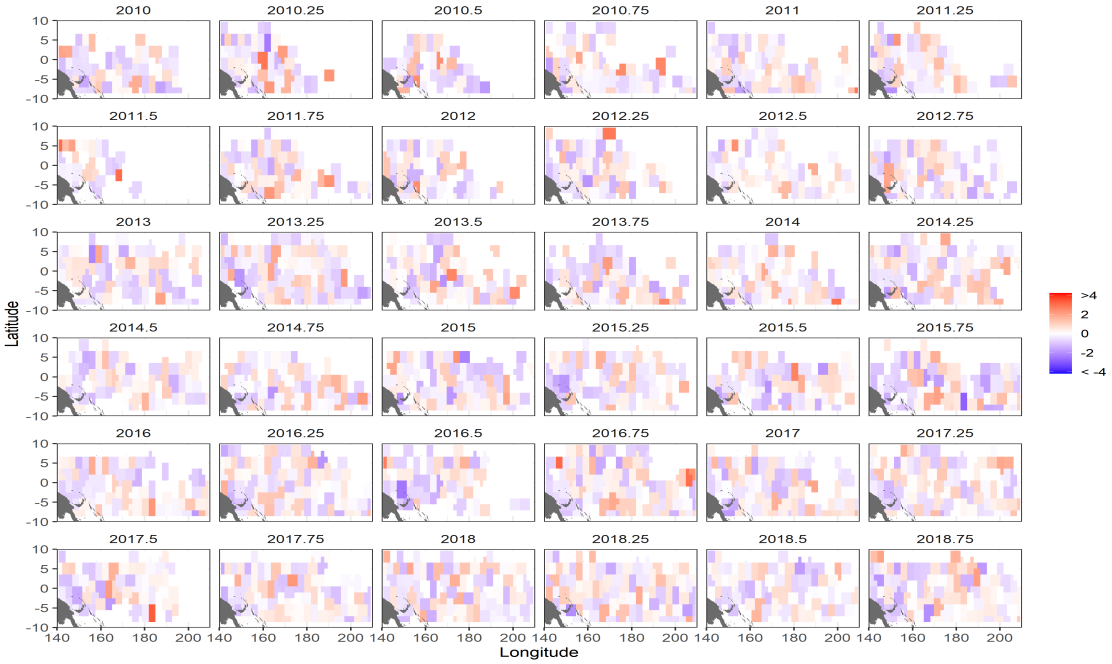

Figure A.16: Mean Pearson residuals, by (1° x 1°) extrapolation grid cell, for the positive catch rate model component.

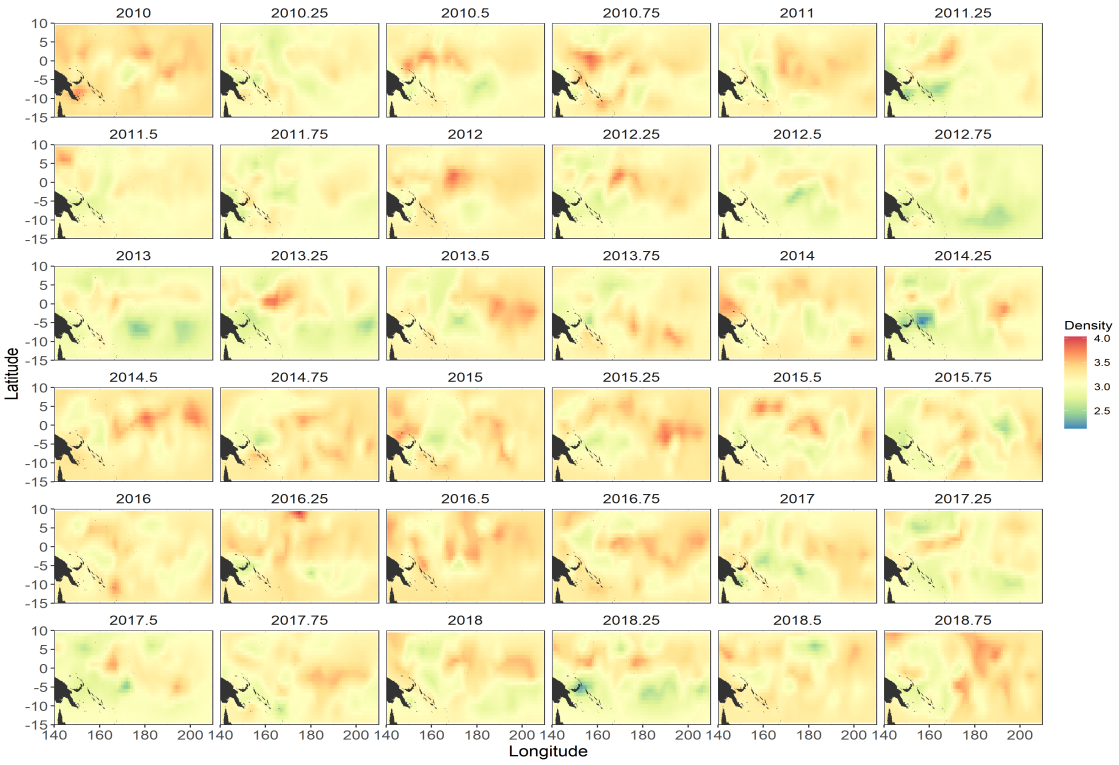

Figure A.17: Illustration of the variability in predicted skipjack relative density across space and through time.

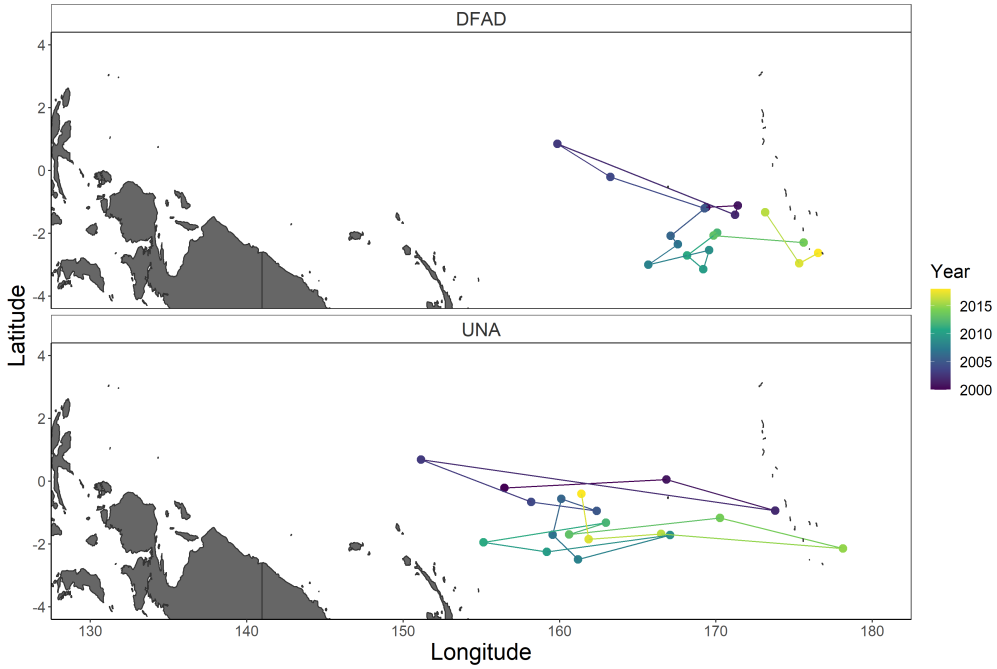

Figure A.18: Center of gravity estimated from the distribution of purse seine skipjack catches, from 2000-2018.

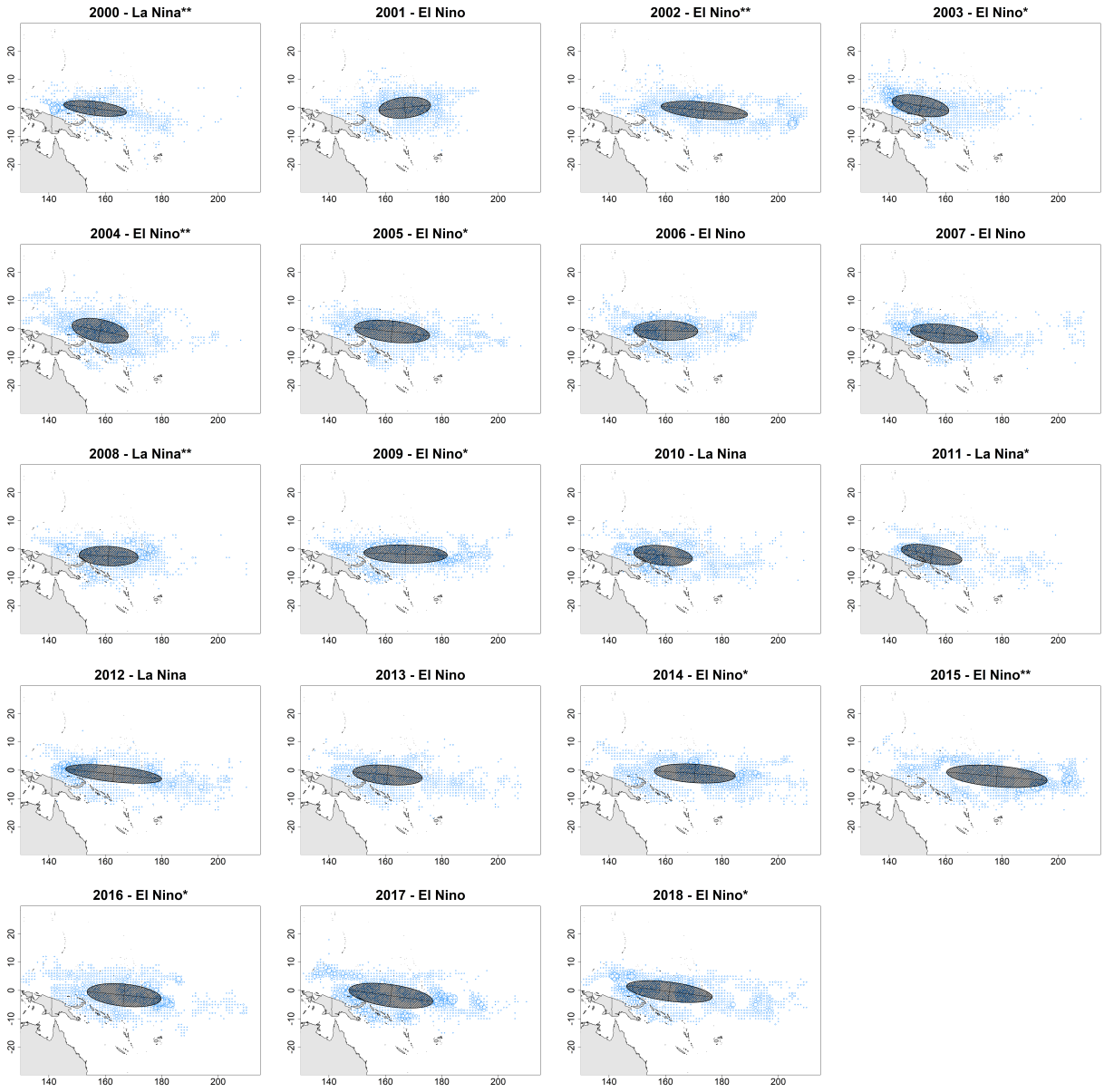

Figure A.19: Center of gravity and inertia of skipjack population from free-school (UNA) sets, 2000-2018. The asterisks indicate relative strength of the ENSO phase, where no asterisk represents a fairly neutral phase, and increasing number of asterisks represents increased strength of the phase.

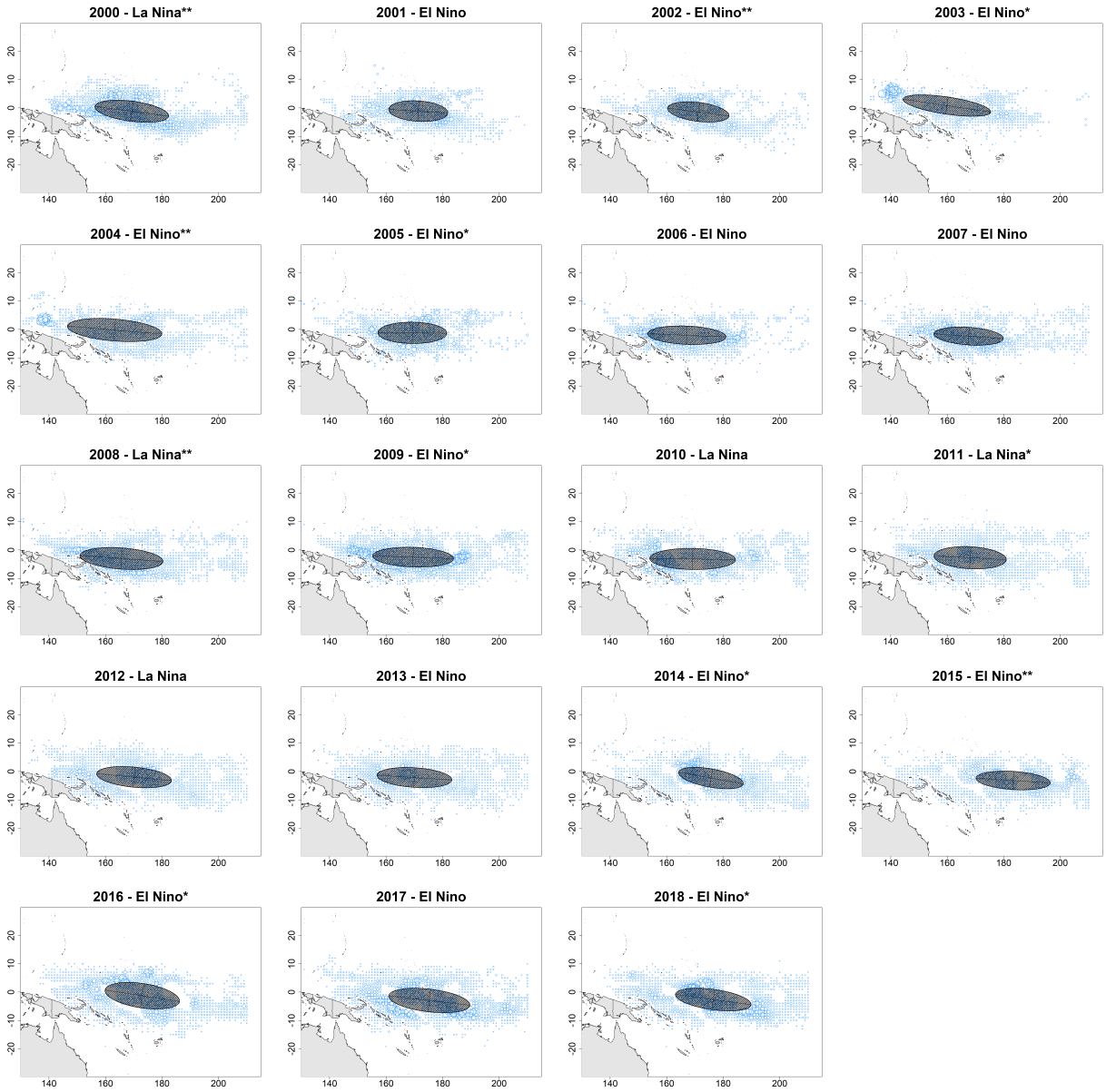

Figure A.20: Center of gravity and inertia of skipjack population from dFAD sets, 2000-2018. The asterisks indicate relative strength of the ENSO phase, where no asterisk represents a fairly neutral phase, and increasing number of asterisks represents increased strength of the phase.